ELR-based biopolymers releasing Kv1.3 blockers for the prevention of intimal hyperplasia: an *in vitro* and *in vivo* study

Sara Moreno-Estar [a, 1], Sofía Serrano [b,1], Marycarmen Arévalo-Martínez [a], Pilar Cidad [a], José Ramón López-López [a], Mercedes Santos [b], M. Teresa Pérez-Garcia [a, 2, *] and F. Javier Arias [b, 2]

[a] Departamento de Bioquímica y Biología Molecular y Fisiología and Instituto de Biología y Genética Molecular (IBGM), Universidad de Valladolid, and CSIC, Spain

[b] BIOFORGE (Group for Advanced Materials and Nanobiotechnology), CIBER-BBN, Universidad de Valladolid, Spain

[1] equal first authors

[2] equal senior authors

Running title: ***PAP-1 releasing ELR-hydrogels against intimal hyperplasia***

* **Corresponding author:**

M. Teresa Pérez García, MD, PhD

Departamento de Bioquímica y Biología Molecular y Fisiología,

Universidad de Valladolid,

Edificio IBGM, c/ Sanz y Forés, 3,

47003 Valladolid, Spain.

Email tperez@ibgm.uva.es

Abstract

Coronary artery disease is the most common cardiovascular disorder. Vascular surgery strategies for coronary revascularization (either percutaneous or open) show a high rate of failure because of restenosis of the vessel, due to phenotypic switch of vascular smooth muscle cells (VSMCs) leading to proliferation and migration. We have previously reported that the inhibition of Kv1.3 channel function with selective blockers represents an effective strategy for the prevention of restenosis in human vessels used for coronary angioplasty procedures. However, delivery systems for controlled release of these drugs have not been investigated. Here we tested the efficacy of several formulations of elastin like recombinamers (ELRs) hydrogels to deliver the Kv1.3 blocker PAP-1 in various restenosis models. The dose and the time course of PAP-1 release from ELRs click hydrogels was able to inhibit human VSMC proliferation *in vitro* as well as remodeling of human vessels in organ culture and restenosis in *in vivo* models. We conclude that this combination of active compound and advanced delivery method could improve the outcomes of vascular surgery in patients.

Key words: vascular smooth muscle cells; intimal hyperplasia; elastin-like recombinamers;,hydrogels; Kv1.3 channels; local drug delivery,

Introduction

Cardiovascular disease is the leading cause of death and disability in developed countries. More than 4 million Europeans die of cardiovascular disease every year, (51% of all deaths among women and 42% among men) and many more require hospitalization after acute episodes or life-long treatments. While mortality rates tend to decrease, the burden of morbidity trends upward since the early 2000s [1]. The development of catheter-based endovascular interventions, with or without stent implantation has represented a huge therapeutical improvement. A limitation of these procedures is restenosis of the target vessel. Mechanical or chemical injury promotes dedifferentiation of the vascular smooth muscle cells (VSMC) of the vessel wall, triggering a proliferative, migratory and secretory phenotype directed to neointima formation [2]. This process of phenotypic modulation (PM) represents the arterial repair mechanisms devised for healing, but an excessive, uncontrolled response leads to an intimal hyperplasic (IH) lesion that renarrows the lumen. Drug-eluting stents for local release of anti-proliferative agents (i.e., placlitaxel, rapamycin) decrease restenosis, but they also block endothelial cell growth, delaying healing and creating late in-stent thrombosis, which is often fatal [3]. Anti-coagulant therapies cannot completely prevent stent thrombosis, and they are associated with high costs and bleeding problems. Moreover, compromised stents cannot be replaced, so that a secondary, invasive revascularization such as bypass surgery is often required. These observations call for the development of anti-restenotic therapies, via innovation in both drugs and delivery methods.

Despite the advancements of endovascular interventions (e.g. stent and/or balloon placement), the coronary artery bypass graft (CABG) remains the standard of care for patients with complex lesions, and is the most frequently performed surgical intervention for relieving consequences associated with ruptured or occlusive coronary artery atherosclerotic plaques [4]. Surgery uses undiseased vessel (most often saphenous vein, internal mammary artery, or radial artery) for diversion of blood from the aorta to the coronary artery, thereby revascularizing cardiac tissue. Open surgery induces trauma to the vasculature associated with inflammation, thrombosis or VSMC proliferation and IH development [5], so that long term efficacy of bypass grafts, especially venous grafts, remains restricted due to restenosis of the conduits. Though arterial grafts exhibit superior patency rate, shapenous vein is most commonly used as it is easier to harvest, and its length allows for making of multiple grafts. However, up to 50% suffer failure within 10 years [6]. Anti-restenotic strategies using either systemic or local drug application have been explored, and the superiority of local drug delivery system was demonstrated (reviewed in [7]). However, the overall outcome of the clinical trials is poor, and an efficient system is not yet available in the clinical routine. Again, both the selection of effective compound(s) and the design of the system need to be considered together in order to improve efficiency of these therapies.

We have previously demonstrated that PM of VSMCs associates with an increased functional expression of Kv1.3 channels [8]. The use of genetic or pharmacological blockers of Kv1.3 channels decreased VSMC proliferation and migration and prevented IH in human vessels and animal models [9–11]. These results identified the use of Kv1.3 selective blockers such as margatoxin (MgTx) or PAP-1 (5-(4-phenoxybutoxy)psoralen) [12] as a novel treatment for vascular diseases associated with PM of VSMC. However, for these drugs to be used as effective therapies in the clinics, we need to explore delivery systems and/or scaffold materials with adequate physicochemical properties, suitable for local application of the blockers with a sustained release at effective concentrations and with a good biocompatibility.

Elastin-like recombinamers (ELRs) are recombinant elastin-mimetic polymers inspired in natural elastin that have been widely investigated as candidates for a broad range of applications from tissue engineering to nanovaccines [13]or drug delivery systems [14,15]. The recombinant DNA technology allows to bioproduce them with totally controlled composition. Moreover, these tailored polymers can include different bioactive sequences and exhibit great biocompatibility, excellent mechanical properties (similar to those of natural elastin), self-assembly capability and a fully reversible thermosensitive behavior. ELRs catalyst-free click hydrogels can be produced under physiological conditions in an efficient, selective and cell-friendly process. Due to their thermo compatibility, these click hydrogels have been excellent candidates for the fabrication of coated vascular stents by injection molding [16,17] or layer-by-layer dip-coating technics [18]. Although very promising results have been obtained in vitro[18], the unreactive nature of these hydrogels needs to be tested in vivo. In addition, these ELRs coatings represent a good strategy for the development of a next generation of drug-eluting stents, by incorporating active anti-restenotic compounds, which could be released locally at the injured vessel. On the other hand, drug loaded ELRs chemical hydrogels have been also used as advanced delivery systems as they have proved to be promising in diseases as rheumatoid arthritis [19], cancer [20] or ischemia [21], showing also versatility in the embedded drug with released control at the right side. So, drug loaded ELRs catalyst-free click hydrogels look particularly promising as advanced drug delivery devices paving the way for future biomedical applications

Combining all these previous evidences, here we explore the efficacy of several formulations of a novel ELR-hydrogel incorporating the Kv1.3 blocker PAP-1 for the prevention of intimal hyperplasia *in vitro* and *in vivo* and using both animal models and human VSMCs and vessels. ELRs biopolymers containing PAP-1 were used as grid-coating or as lyophilized hydrogel beads and the time-course of PAP-1 release was explored in cultured VSMCs or in vessel rings in organ culture. In addition, the effect of injectable ELR-hydrogels containing PAP-1 for the prevention of IH in an animal model of vascular injury was studied. Our results confirm the efficacy of PAP-1 embedded ELR-hydrogel for the prevention of vessel remodeling both in vitro and in vivo.

Materials and methods

Synthesis, expression and purification of the ELRs.

The ELRs used in this work were obtained by using standard genetic engineering techniques. They were biosynthesized in a 15-L bioreactor and later, purification was performed with several cycles of temperature-dependent reversible precipitations, by centrifugation below and above their transition temperature (Tt), making use of the intrinsic thermal behavior of these compounds [14]. The ELRs were subsequently dialyzed against purified water and freeze-dried. Two different ELRs were obtained: VKV and IK. The amino-acid sequences of these polymers are:

VKV: MESLLP VG VPGVG $[VPGKG(VPGVG)_5]_{23}$ VPGKG $(VPGVG)_4$

IK: MESLLP $[(VPGIG)_2(VPGKG)(VPGIG)_2]_{24}V$

The purity and chemical characterization of these ELRs were verified by sodium dodecyl sulfate polyacrylamide gel electrophoresis (SDS–PAGE), matrix-assisted laser desorption/ionization time-of-flight (MALDI-TOF), amino acid composition analysis, differential scanning calorimetry (DSC) and nuclear magnetic resonance (NMR) [14]. NMR and MALDI-ToF analysis have been carried out in the laboratory of Instrumental Techniques (LTI) Research Facilities of the University of Valladolid.

Chemical modification of the ELRs

ELRs were chemically modified by transformation of the ε-amine group from lysine to bear cyclooctine and azide reactive groups respectively, as reported previously [16,22]. VKV was dissolved in dimethylformamide (DMF, Sigma) at final concentration of 0.05 g/mL at room temperature (RT) for 1 h under inert atmosphere. Then, bicyclo [6.1.0] non-4-yn-9-yl-methyl N-succinimidyl carbonate (0.6 eq., Mw 291.30 g/mol, GalChimia, A Coruña, Spain) was dissolved in DMF and was added to the ELR solution at final concentration of 3.3 mg/mL. The resulting mixture was stirred for 48 h at RT in argon atmosphere. The modified VKV was purified by precipitation with diethyl ether; the supernatant was removed, and the white solid washed with acetone (3 times) and dried under reduced pressure. The solid was re-dissolved in cold ultrapure MQ water at 4°C, dialyzed against MQ water and filtered through 0.22 µm filters (Nalgene) giving rise to a sterile solution that was freeze-dried prior to storage.

The same procedure was used to modify IK with an azide group. In this case, 2-Azido ethyl (2, 5-dioxopyrrolidin-1-yl) carbonate (1 eq, Mw 228.17 mg/mmol, GalChimia, A Coruña, Spain) was dissolved in DMF and added to the IK solution at final concentration of 1.3 mg/mL. Purification of modified IKx24 was carried out as described above.

The modified biopolymers VKV-cyclooctine renamed VKV-CO and IK-azide renamed IK-N3 were characterized by MALDI-ToF, NMR and Fourier transform infrared spectroscopy (FTIR-ATR). MALDI-ToF and ^{1}H-NMR (in DMSO-d6) allowed us to assess the degree of lysine modification (Supporting information).

Hydrogel formation

Gels were formed by catalyst free click reactions between an azide group and an activated alkyne as cyclooctine group from both modified ELRs chains. Solutions of VKV-CO and IK-N3 were prepared in purified water at 100 mg/ml and kept at 4°C for at least 24 h. In PAP-1 loaded gels, the necessary quantity of 26 mM of PAP-1 in DMSO will be added to both solutions to get a final concentration of 1mM. 1) Covered grids (Square 50 Mesh Tabbed Grids Nickel, Agar Scientific AGG2905N) used as mimetic DES [18] were obtained by dip-coating alternating the solutions of IK-N3 and VKV-CO, kept at 4°C in two separate containers, sequentially immersing the device first in the solution with IK-N3 and then in the VKV-CO solution [18]. This step is repeated 10 times for each of the solutions, with 5 min gaps between each layer to allow the cross-linking of the azide group of one layer and the cyclooctine group of the next layer. The macroscopic examination was realized with a Leica DMS 1000 digital microscope system. 2) Hydrogel beads were obtained mixing equal quantity of the ELR solutions (VKV-CO: 20 µL, IK-N3: 20 µL) at 4 °C, and immediately placed a quantity of the mixture (30 µL) on a flat surface at 37°C. After 5 min at 37°C, the gel beads were completely formed.

In vitro PAP release studies

Experimental procedure

Release experiments were performed using the sample-drawing procedure. The covered grids were placed in a 2 mL vial and 100 µL of tempered aqueous delivery medium was added and, at predetermined time intervals (1, 2, 7, 14, 21, 30, 60, 90 days), the solution was completely removed to measure PAP-1 concentration and new tempered solution was added. This study was conducted over 90 days. With the aim of determining the real amount of PAP-1 contained in the covered grids, two of them were placed in a 2 mL vial with 100 µL of DMSO and were subjected to the same procedure as the real aqueous release. In this case, the delivery time was extended to 121 days in order to ensure that all PAP-1 had been released.

The concentration of PAP-1 in the released medium was determined by Ultra Performance Liquid Chromatography (UPLC, Waters Acquity UPLC system and BEH C18 (1.7 µm, 2.1 x 50 mm) column with a Nova-Pak C18 (2.1 x 10 mm) cartridge) in the LTI Research Facilities. The mobile phase is Acetonitrile:H_2O with 0.1 % formic acid and 0.6 mL/min flow rate. The delivery medium was evaporated for 20 min in the Speed Vac (Thermo Scientific, Savant SpeedVac Kit OP230V). Then, 0.5 mL of methanol was added and sonicated for 10 min in the ultrasound for the total dissolution of the PAP-1. All experiments were performed in triplicate .

Mathematical models description

To explore the release kinetics of PAP-1 *in vitro*, , release profiles were analysed using two mathematical models, as described below.

The Lindner and Lippold equation explains the drug release through a polymeric matrix as a diffusion process. The equation includes a parameter ‘b’ which represents the burst effect and k_1 represents the Fickian diffusion constant

$$\frac{M_t}{M_\infty} = k_1 \cdot t^n + b \qquad (1)$$

The biexponential Peppas–Sahlin equation [23] was also used to determine the contribution to the drug delivery of both the Fick diffusion process and relaxation of the polymer chains irrespective of the geometry of the release system.

$$\frac{M_t}{M_\infty} = k_1 \cdot t^n + k_2 \cdot t^{2n} \quad (2)$$

Here, n is the Fick diffusion exponent for a release system with any geometrical shape, k_1 represents the Fickian diffusion constant and k_2 represents the polymer chain relaxation constant.

Morphological characterization by Scanning Electron Microscopy (SEM).

Hydrogel structure and morphology were evaluated by SEM. ELR-hydrogels were immersed in MQ water at 37°C for 1 day. Hydrated gels were dropped into liquid nitrogen, physically fractured and immersed in liquid nitrogen again before finally being freeze-dried. Images of lyophilized hydrogels were obtained by SEM (JEOL, JSM-820), with no prior coating procedures. Morphological details such as pore size, % of porosity and swelling ratio were quantified as previously described [16].

Mechanical properties characterization by rheological studies.

The mechanical properties of the hydrogels were studied using rheological test in a strain-controlled AR-2000ex rheometer (TA Instruments) equipped with a Peltier plate temperature control. A stainlesssteel plate with a diameter of 12 mm and a gap of about 1000 microns between the plates was adjusted. Measurements were carried out at 37°C, with the sample temperature being controlled and maintained with the Peltier device.

The dynamic shear modulus of the hydrogel was characterized using previously a strain and frequency sweep. The range of strain in which the gels exhibited a linear region of viscoelastic properties was determined via a dynamic strain sweep (with amplitudes between 0.1 and 30 %) carried out at a frequency of 1 Hz to measure the dynamic shear modulus as a function of strain. Then, a frequency sweep between 0.01 and 70 Hz was performed at a fixed strain 1 % (corresponding to the hydrogel linear region).

Finally, with the results obtained from the previous studies, a stress relaxation test was carried out with the objective of evaluating the mechanical behavior of the hydrogels. These experiments were performed within the linear viscoelasticity region, where storage (G') and loss (G'') moduli are independent of the stress magnitude. In our measurements, a final time of 300 s was selected in order to determine long-term hydrogel behavior.

Rheological measurements provide the storage modulus (G') and the loss modulus (G'') and complex viscosity magnitude as a function of strain or frequency at a fixed temperature. Three different hydrogels were tested (n = 3).

Human samples

Human mammary arteries (hMA) and human saphenous veins (hSV) from COLMAH (**COL**ección de **M**uestras **A**rteriales **H**umanas) collection (https://www.redheracles.net /plataformas/en_coleccion-muestras-arteriales-humanas.html) were obtained from donors undergoing heart bypass surgery at the Clinic Hospital of Valladolid, with the written informed consent obtained from each participant. The sample collection and the study were approved by the Hospital Ethics according to the standards of the Helsinki Declaration. The vessels were

collected in culture medium (DMEM/F-12 with HEPES Buffer) and used in the next 24 hours for organ culture or for obtaining VSMCs cultures

Primary VSMCs cultures

VSMCs were obtained from explants of vessels and maintained as previously described [24]. Briefly, after removing the adventitia and endothelial layers, the media layer was cut into 1-3 mm fragments. After washes with sterile PBS in a laminar flow cabinet, the fragments were placed (close to each other to facilitate paracrine stimulation) in Petri dishes coated with Cultrex® Basement Membrane Matrix (Trevigen) and incubated in Minimal Essential Medium (MEM, Gibco) supplemented with 20% fetal bovine serum (FBS), 100 U/ml penicillin, 100 U/ml streptomycin, 5 µg/ml fungizone and 2 mM L-glutamine, at 37°C in a 5% CO2 humidified atmosphere. Migration and proliferation of VSMCs from explants was visible within 1-2 weeks. Once VSMCs reached confluence, they were tripsinized and seeded again at 30-50% confluence in SMC P-STIM medium (MEM with 10% FBS, 5µg/ml insulin, 1 ng/ml bFGF, 5 ng/ml EGF, 100 U/ml penicillin, 100 U/ml streptomycin, 0.25 µg/ml fungizone and 2 mM L-glutamine). VSMCs in passages 3-9 were used for proliferation

Proliferation assays.

The percentage of cells at the S phase was quantified using EdU (5-ethynyl-2´-deoxyuridine) incorporation for 6h with a commercial kit (Click-iT® EdU Imaging Cell Proliferation Assay, Invitrogen) as described [11]. Briefly, 25,000 VSMCs were seeded onto fibronectin-coated coverslips placed in 12 mm wells with control media (10% FBS). Next day, media was replaced with serum-free (SF) media, and proliferation was induced by addition of PDGF (20 ng/ml), alone or in the presence of PAP-1 (100nM) or ELR-containing-PAP- during 24 h. Triplicate samples were used, and controls were included in all experiments. Proliferation was determined as the percentage of EdU positive cells (EdU+) from the total cell number stained with Hoechst, obtained from the average of 4 randomly selected images per coverslip, captured using the 4X objective in a Nikon Eclipse 90i microscope. ImageJ (Fiji) software was used to analyze the images in a blind manner.

Organ culture of human saphenous veins

For organ culture experiments hSV were cut in 5mm rings, placed in MEM culture medium (Gibco) supplemented with penicillin-streptomycin (100U/ml each), 5µg/ml Fungizone and 2mM L-glutamine and kept for 2 weeks at 37ºC in 5% CO2 humidified atmosphere. 20% Fetal Bovine Serum (FBS) was added to induce intimal hyperplasia (positive control), while FBS-free medium was used as negative control. Experimental conditions include the addition of the Kv1.3 blocker 5-(4-phenoxybutoxy) psoralen (PAP-1) in the 20%FBS medium or in the different ELR formats (grids or beads) as indicated. Media was changed every 3 days. In all cases, sequential sections of the same vein were used for the different experimental conditions.

In vivo model of lesion

Carotid artery ligation was carried out in BPH mice (Jackson Laboratories) to induce intimal hyperplasia (IH). Mice were anesthetized with 2% isoflurane using SomnoSuite® (Kentscientific). The right carotid artery was ligated distal to the carotid bifurcation. Carotid ligation was carried out in three different groups of animals: 1) Control animals in which no other procedure was carried out (n=5); 2) Animals with systemic treatment, in which two days prior to carotid ligation, an osmotic minipump (model 2004, Alzet), containing either PAP-1 (50

µg/Kg/day) or vehicle (PEG-35 castor oil,25% in H_2O, Kolliphor® EL, Sigma) was implanted subcutaneously in the dorsal region of the neck (n=6 in each group) ; and 3) Animals with local treatment, in which control ELR or PAP-1-ELR containing gels formed "in situ" by catalyst free click reactions were applied surrounding the ligation area (n=6 per group).

Ibuprofen (20 mg/100 ml in the drinking water) was administered for 3 days after surgery. After 28 days mice were euthanized in CO_2 chamber to collect right (ligated) and left (control) carotid arteries, that were fixated overnight in 4% formaldehyde. All procedures were approved by the Institutional Care and Use Committee of the University of Valladolid in accordance with the EU Directive 2010/63/EU for animal experiments. Both male and female BPH mice were used as detailed below.

Morphometric analysis

hSV rings in organ culture and mice carotid arteries were embedded in paraffin to obtain 7-µm thick sections. Morphometric analysis was performed with Masson trichrome stained sections, as described elsewhere [11] and analyzed blinded using computerized morphometry (ImageJ). Measures included luminal, intimal, media and vessel area. From these data, the wall area (intima+media area), the intima to media ratio (I/M ratio) and the percentage of stenosis were calculated to define the degree of vessel remodeling [25].

Statistical analyses

Data were plotted and analyzed using Origin and Excel software. Pooled data are expressed as mean ± SEM, and p-values < 0.05 were considered as significantly different. For comparisons between two groups, normal distribution and equal variance were assessed with Shapiro-Wilk test and Bartlett test, respectively. In the case of normality, p-values were determined with Student´s t test for paired or unpaired data as required, otherwise Wilcoxon or Mann-Whitney tests (for paired or unpaired data respectively) were applied. For comparisons among several groups, ANOVA followed by Tukey test was employed in the case of normal distributions. If not, Kruskal-Wallis analysis followed by Dunn test was used. R-studio and Excel were used for statistical analyses.

Results

Production, chemical modification and characterization of the ELRs

Two different ELRs (VKV and IK) were chemically modified through their lysine residues to incorporate different reacting groups (IK bearing azides and VKV bearing cyclooctines), as described in the material and methods section. The characterization of both modified ELRs was carried out by MALDI-TOF, NMR, FTIR and DSC (see supporting information).

VKV was chemically modified by amidation reaction of amine groups present in the side chain of lysine amino acids with an N-succinimidyl carbamate derivative carrying a cyclooctine group. Thirteen lysines of the 24 total ones were modified as determined by the increase in molecular weight recorded by MALDI-ToF technic (Figure S1) and corroborated by integral analysis from NMR signals (Figure S2). The number of modified lysines, equal to the number or cyclooctine groups introduced at the VKV-CO molecule, for 0.6 equivalents of reactant is in accord with a 92% conversion yield.

In a similar way, IK was chemically modified also by amidation reaction of lysine amine groups, this time using an N-succinimidyl carbamate derivative carrying an azide group. Twenty lysines of the 24 total ones were modified and an 83% conversion yield was obtained for one equivalent of reactant. The percentage of modification was determined as previously explained for VKV-CO (Figure S3 and S4) and, additionally, the presence of azide groups was corroborated by their characteristic FTIR band at 2100 cm^{-1} (Figure S5).

PAP-1 embedded hydrogels formulations

In order to explore the combination of an active compound as PAP-1 with ELRs hydrogels as release devices, two different approaches have been followed leading to several formulations for restenosis models. On the one hand, nickel grids as implantable coronary stent prototyping models [17] were coated using layer-by-layer strategy, (LbL), with PAP-1 embedded click hydrogel. On the other hand, PAP-1 containing hydrogel beads for *in vitro* analysis and *in situ* injectable hydrogels for in vivo experiments were prepared following the “copper-free click hydrogels” methodology previously described by us [15].

The layer-by-layer strategy consists of alternatively dip-coating with differently functionalized ELRs, IK-N3 and then VKV-CO for one bilayer, covering the grid with five bilayers connected to each other by click reaction between azide and cyclooctine groups (Figure 1A). The resulting Click-ELR film uniformly filled the whole grid as was checked by macroscopic examination (Figure 1B). The presence of PAP-1 at ELRs starting solutions led to PAP-1 coated grids simulating an implantable device such as a drug eluting stent (DES). The PAP-1 embedded in the coating was estimated by weight difference between uncovered and coated grid considering that PAP-1:polymer mass ratio is known.

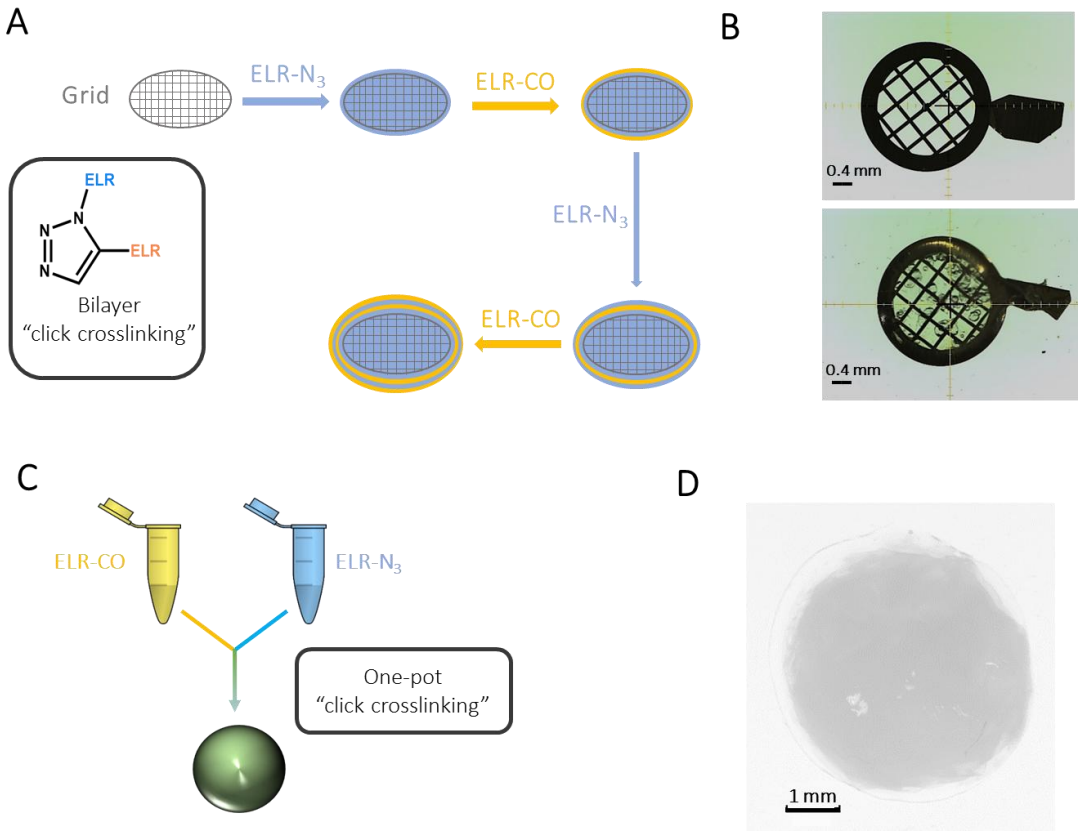

Figure 1. ELR-hydrogels formulation and characterization. A. Procedure for the fabrication of the click-ELR covered grid, showing the scheme of the Layer-by-Layer methodology, in which the grid is sequentially immersed in the solution of IK-N3 + PAP-1 and VKV-CO + PAP-1 to create a crosslinked ELR-covering film; **B.** Microphotograph of an uncovered and covered grid. Scale bars: 0.4 mm. **C.** The scheme depicts the injectable click-ELR hydrogel beads, representing the "copper-free click" hydrogels preparation methodology. Hydrogel beads were obtained mixing equal quantity of the ELR solutions at 4 °C, and immediately placing 30 µL of the mixture on a flat surface at 37°C. **D.** Microphotograph of a hydrogel bead obtained with this method. Scale bar: 1 mm.

In situ injectable hydrogels were prepared from embedding of PAP-1 in both differently functionalized ELRs solutions at low temperature (4ºC). The injection of the mixture at the injured vessel in an in vivo animal model lead to the formation of a stable well-integrated hydrogel as a store for PAP-1. Hydrogel beads were obtained following the same "copper-free click" hydrogels preparation methodology [16] (Figure 1C) by adaptation to small volumes of ELRs solution mixtures (Figure 1D), resulting in 5 mm diameter semi-spheres. The volume of ERLs and PAP-1 solutions employed is the one containing the same estimated mass covering the coated grids in order to embed the same amount of PAP-1. Thereby, the results obtained in in vitro studies can be compared between the two strategies since the amount of drug is similar.

Click hydrogels characterization

Morphology and mechanical properties of PAP-1 embedded click hydrogels were characterized to prove their analogy with extracellular matrix since they are going to be injected to form 3D scaffolds for PAP-1 gradual delivery.

The morphology of the hydrogel was investigated by scanning electron microscopy and ELRs hydrogels at 100 mg/ml show variability in pore sizes ranging from 3 to 20 µm with an internal interconnected structure. The porosity value is found to be 88 % with a swelling ratio of 1.6 % at 37ºC. Those values are similar to those for analogous click hydrogels previously used as injectable in situ cross-linkable scaffolds for regenerative medicine [26].

Rheological measurements in the linear viscoelastic range will allow us to determine the viscoelastic mechanical properties of the hydrogel, thus providing information in conditions close to hydrogel stability [27–29]. Variation of the linear viscoelastic range was measured rheologically in hydrogels at a concentration of 100 mg/mL as those used in *in vivo* experiments and in triplicate. The linear viscoelastic region of the hydrogel was determined by using strain sweep and frequency sweep measurements. G´ and G´´ were found to remain independent of the strain amplitude (linear viscoelastic behavior) up to values of about 10% and at a fix frequency of 1Hz; in the same way, G´ and G´´ were found to remain independent of the frequency up to 7-8 Hz at a fix 1 % strain. In order to ensure that measurements were carried out within the linear viscoelastic region, every subsequent rheological tests were performed for 1% strain and 1 Hz of frequency.

Focusing on a fixed % strain of 1% and frequency of 1 Hz, G' and G'' values are represented in figure S6. The gel strength can be estimated from the magnitude of G' and the significant difference between G' and G'' (G' >> G''), which means that the storage modulus is the major contributor. At 1 Hz, the value of G' and G´´ is around 220 Pa and 13 Pa, respectively. The quotient between G´ and G´´ gives us the value of the loss tangent (tg δ) where δ represents the lag between the stress and the deformation; being a parameter indicative of the relationship between the energy dissipated and the stored one by the material, and so a measure of viscoelasticity behavior. In this case, a value of δ close to zero (0.06) and kept constant with time indicates that is an elastic material. The hydrogel can be classified as soft material displaying a high degree of elasticity rested on their elastin inspiration and well suited for application in vascular lesions.

Release and mathematical model

With the aim of studying the delivery behavior of PAP-1 from grid coatings, an *in vitro* kinetic release study was performed. The in vitro PAP-1 release curve is shown in Figure 2A and represents the concentration of PAP-1 released from hydrogel grid coating over 90 days (experiments were performed in triplicate). As shown in the figure, an initial quantity of 1262 nM was released during the first 7 days corresponding to a 0.5 % of total cargo. This total cargo was determined by parallel PAP-1 in vitro release assays using DMSO as solvent (see supporting information, figure S7). In a second stage, from 7 to 30 days, the release rate decreased and only an average of about 190 nM was delivered for each period of seven days. Between 30 and 90 days, a third stage occurred with an even lower release rate that delivered less than 50 nM on average per seven days. The kinetics of PAP-1 release resembles he behavior of this drug in natural tissues.

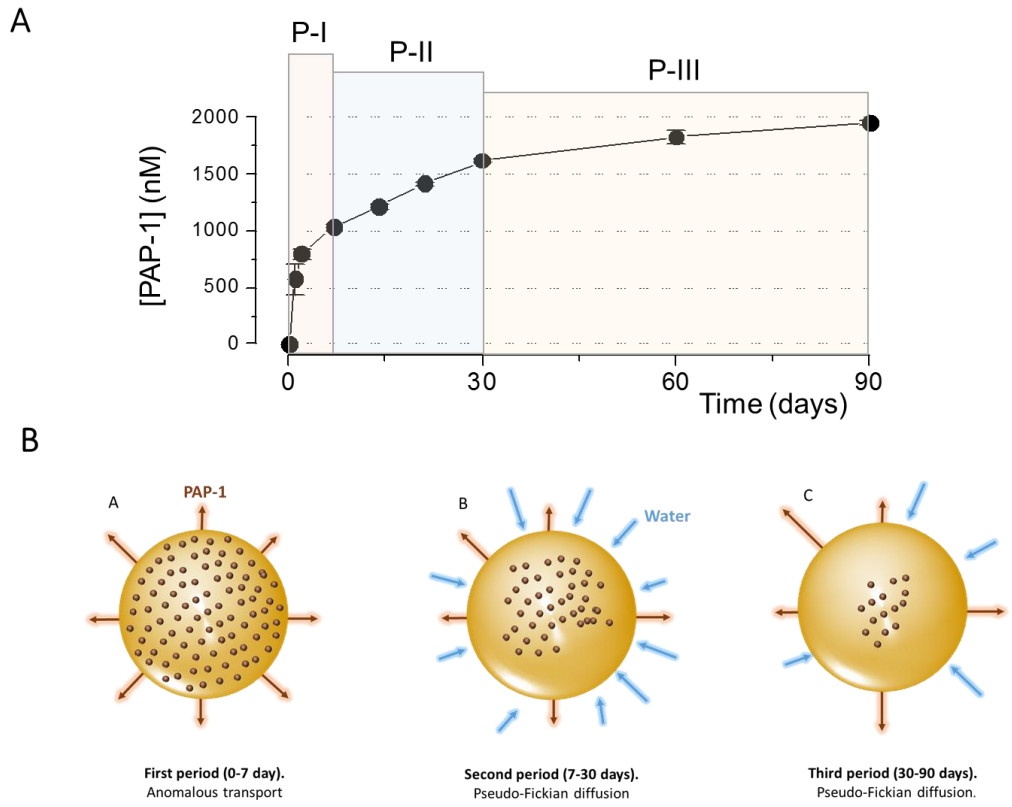

Figure 2.In vitro release of PAP-1 from ELR-hydrogel A. Time course of the PAP-1 released from covered grids. Grids were placed for up to 90 days at 37°C and 60 rpm in 100 µL distilled H_2O, and cumulative PAP-1 release (in nM) was determined by UPLC at the indicated points. Each data point is the mean ± SEM of 3 independent determinations. The line shows the fit by eye of the data. To analyze the kinetics of the release, the profile was divided in three periods (P-1 to P-III) as indicated by the colored areas. **B.** Diagram of the PAP-1 delivery kinetics showing the first period of anomalous or non-Fickian diffusion, followed by a second period of lower pseudo-Fickian diffusion mechanism which depends on the diffusion of PAP-1 through the swollen porous polymer matrix. The third period shows an even lower pseudo-Fickian diffusion as PAP-1 remains in the innermost layers and it takes longer to cross the hydrogel layer that separates it from the outside (see text for more details).

In order to understand the relation between the dug-delivery process and the release kinetics obtained from in vitro experiments, the experimental profile was mathematically fitted with the models exposed in material and methods. The release profile was divided in three periods as has been noted above (between 0 and 7 days, from 7 to 30 days and from 30 to 90 days) to make more accurate adjustment of the process. As it is shown in table I, the best fitting was obtained for Peppas-Sahlin equation what indicates a preferred diffusion mechanism for PAP-1 release, and, the fact that $k_1 >> k_2$ indicates that the release is little influenced by the relaxation of the polymer chains. Moreover, a coefficient *b* (burst effect) in the Lindner-Lippold equation close to zero suggest that PAP-1 quantity at the surface of hydrogel is insignificant.

	Peppas-Sahlin				Lindner-Lippold			
Periods	k_1	k_2	n	R^2	k_1	b	n	R^2
I (0-7 day)	31,594	-5,138	0,643	0,999	28,473	-0,077	0,272	0,992
II (7-30 day)	21,990	5,997	0,220	0,995	27,553	0,151	0,286	0,994
III (30-90 day)	29,445	-2,060	0,335	0,996	30,063	-0,597	0,253	0,993

Table I.- *Fitting of PAP-1 release profile from covered grids to the Peppas-Sahlin and Lindner-Lippold equations.*

The power law release exponent (*n*) describes the release mechanism from thin polymer samples like ours. The first period release (0-7 day) would be governed by anomalous or non-Fickian diffusion (0.5 <*n* <1), because of the controlled relaxation of the polymeric chains. In the second and third periods (7-30 and 30-90 days, respectively) *n* is below 0.45, which represents a pseudo-Fickian diffusion mechanism indicating that the release rate depends on the diffusion of PAP-1 through the swollen porous polymer matrix. In short, drug release is slow due to the hydrophobic interactions between PAP-1 and the polymer matrix and to the low solubility of PAP-1 in aqueous solutions. PAP-1 molecules located in the inner layers of the matrix have more difficulties to reach the release media, being retained since molecules have to pass through each of the pores of the matrix. The delay in PAP-1 release is also influenced by the water absorption mechanism of the hydrogel, exerting an opposite force to PAP-1 delivery (Figure 2B).

Effect of PAP-1 released from ELR hydrogels in cultured VSMCs

We next explored the effect of PAP-1 released from ELR hydrogel beads or covered grids on the proliferation rate of cultured VSMCs. Our previous data indicated that Kv1.3 blockers such as PAP-1 were able to inhibit in a dose-dependent manner the proliferation of VSMC from different vascular beds and species, including human [8,10]. Lyophilized hydrogel beads or covered grids (both with control ELRs or with ELR containing PAP-1) were placed in the wells with VSMCs cultures and PDGF-induced proliferation was measured after 24h treatment and compared with proliferation rate in the absence of ELR (Ctrl) or in the presence of 100 nM PAP-1 in the media. The results of these experiments (Figure 3A,B) show that PAP-1 released from either ELR-covered grids or beads was able to inhibit VSMC proliferation to the same extent than 100n M PAP-1, while in the absence of PAP-1 both devices had no effect on PDGF-induced proliferation. Since 100 nM PAP-1 is a saturating concentration for the inhibition of cell proliferation, these experiments demonstrate that ELR hydrogels release enough PAP-1 to get at least such concentration. In addition, to explore the time course of PAP-1 release from these devices, ELR-PAP covered grids were kept in culture media for different time periods (ranging from 1 to 12 weeks) before they were used for a 24h treatment of VSMCs. As shown in part C of the figure, we did not see differences in the blocking effect of the covered grids that had been previously releasing PAP-1 during up to 12 weeks, indicating that suitable levels of PAP-1 release are maintained for long periods of time.

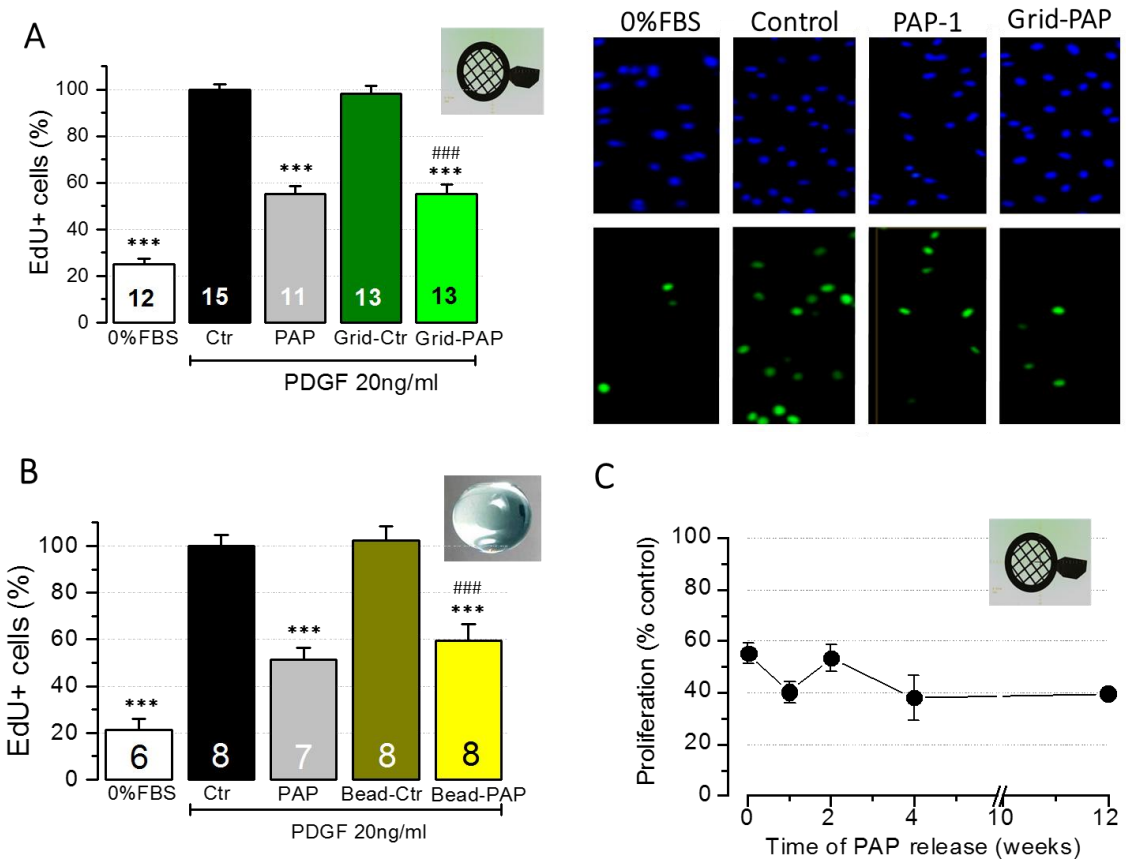

Figure 3. Effect of PAP-1 released from ELR hydrogels in cultured VSMCs **A.** Proliferation of human saphenous vein (hSV) vascular smooth muscle cells (VSMCs) in primary culture was determined by EdU (5-ethynyl-2'-deoxyuridine) incorporation, after a 24-h treatment in serum-free conditions (0% FBS) or in the presence of 20 ng/mL PDGF in the indicated experimental conditions: PDGF alone (Ctrl), plus 100 nM PAP-1 (PAP), or in the presence of grids coated with ELR alone or ELR-PAP-1 (Grid-Ctr and Grid-PAP respectively). Each data bar is mean ± SEM of the indicated number of determinations obtained in at least 6 independent experiments. Positive and negative controls (0% FBS and PDGF 20ng/mL) were included in all experiments, and data was normalized to the proliferation rate observed in control (20 ng/mL PDGF) conditions. ***P<0.001 with respect to PDGF alone; ### ***P<0.001 with respect to Control grid. The right panels show representative images of Hoechst- labelled nuclei (blue) and EdU+ cells (green) from the same fields in the indicated experimental conditions. **B**. The same experimental design as in A was carried out to explore the effect of lyophilized hydrogel beads made of ELR alone (Bead-Ctr) or containing PAP-1 (ELR-PAP). Mean ± SEM of the indicated data points obtained from at least 4 different cell cultures. ***, ### p<0.001 with respect to Ctr (PDGF alone) or Bead-Ctr respectively. **C**. The inhibitory effect on PDGF-induced proliferation of PAP-1 released from ELR-covered grids was explored in another set of similar experiments (EdU incorporation experiments in VSMC cultures treated for 24h with these grids) but in this case the covered grids were kept for the indicated time in culture media before their application to the VSMCs. No statistically significant differences were observed among the different points.

Effect of ELR-PAP hydrogel beads on human vessel remodeling

As PAP-1 released devices are intended for the prevention of IH in human vessels, we next explored their ability to inhibit vessel remodeling in organ culture. We have previously reported that 20% FBS incubation for two weeks led to IH development of human vessels rings in ex-vivo organ culture [11]. This remodeling was characterized by an increased thickness of intimal and media layers together with a decrease of the lumen area and was significantly prevented when 100nM PAP-1 was present in the culture media (see control sections in figure

4). Here we explore in parallel, in sections of the same human saphenous veins (hSV), the effects of incubation for two weeks with control ELR or ELR-PAP hydrogel beads. Our data (Figure 4) indicated that control ELR hydrogel beads did not affect IH, while ELR-PAP beads had the same effect that direct PAP-1 application to the 20%FBS media: We observed an inhibition of vessel remodeling with a reduced neointima formation. This is reflected in the significant decreases of the % stenosis, the % of intima area and the I/M ratio, as represented in the right panels of figure 4. As in the case of cultured VSMCs, the same results were obtained when using ELR covered grids (data not shown)

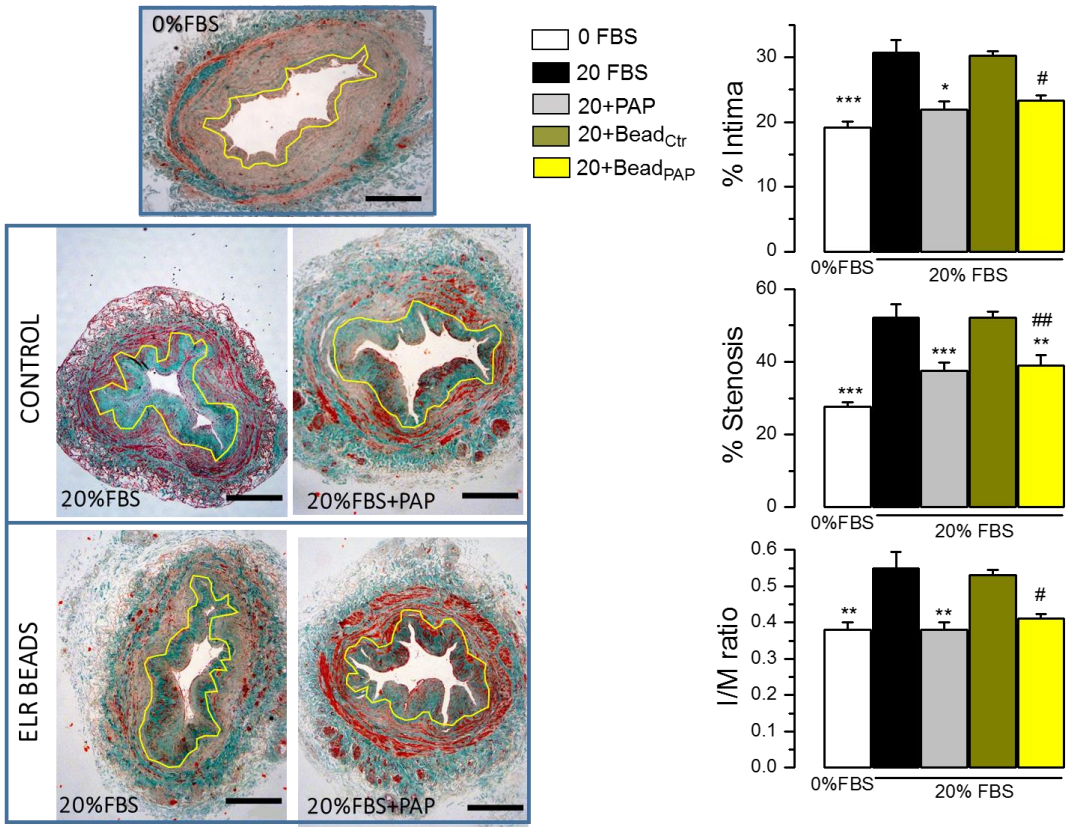

Figure 4. Effect of ELR-PAP hydrogel beads on human vessel remodeling. A., Representative microphotographs of human saphenous vein (hSV) kept in organ culture for 2 weeks in serum-free conditions (0% FBS), or in the presence of 20% FBS alone or combined with PAP-1 (100 nmol/L) in control conditions or in the presence of lyophilized control ELR or ELR-PAP beads as indicated. The yellow line marks the internal elastic lamina which defines the intima/media border. Images were taken with a 4× objective (NA=0.13), scale bars 500 µm. **B**. Remodeling was characterized using several measures as indicated in the plots. The upper plot shows the percentage of the vessel area occupied by the intima layer (%intima); the middle graph shows the degree of lumen stenosis calculated as % stenosis = 100·(Intima area–Lumen area)/Intima area, and the lower plot shows the intima to media ratio (I/M ratio, Intima area/Media area). Each data bar is mean ± SEM of 6-10 different vessels. Positive and negative controls (0% and 20% FBS) were included in all experiments, and vessel rings used for the different conditions were obtained from consecutive vessel segments of similar diameter.* p<0.05; ** p<0.01; *** p<0.001 with respect to 20% FBS. # p<0.05; ## p<0.01 with respect to 20%FBS+bead control.

Effect of ELR-PAP hydrogel in an in vivo model of vascular injury

Finally, we studied the effects of ELR-PAP hydrogels when applied at the injured vessel in an animal model of vascular lesion. Carotid ligation was used to induce IH in mice because it is an easy and reproducible technique. In this model there is a complete disruption of blood flow in the common carotid artery, but the ligated vessel is still subject to arterial blood pressure, and the hemodynamic changes associated to the loss of laminar flow activate formation of neointima [32]. We first checked that carotid ligation produced a consistent and robust IH lesion in all the animals (left panels in figure 5A). The perivascular application of ELR hydrogel (middle panels) around the ligated artery did not seem to modify vessel remodeling, while ligated arteries treated with ELR-PAP hydrogels (right panels) showed a clear reduction in the development of neointima after 4 weeks. In all cases, morphometric analysis showed that carotid ligation induced inward remodeling, with marked increases of the wall thickness/wall area and a concomitant decrease of the lumen area, so we used these descriptors to define remodeling upon ligation. Figure 5B shows the average data obtained when calculating the lumen area (in % of the vessel area) and the wall thickness in all the conditions depicted in figure 5A. The decrease of lumen area in the ligated CA is more pronounced in control conditions or in arteries treated with ELR alone than in the presence of ELR-PAP hydrogels. The effect of PAP-1 treatment is even more clear when determining wall thickness, as no significant change was observed between control and ligated CA in this case (right panel in figure 5B). In addition, both male and female mice were subjected to carotid ligation to investigate possible sex-dependent differences in vessel remodeling. Wall area in ligated CA was 33929 ± 1538 μm^2 in males versus 31148 ± 3096 μm^2 in females, p=0.46, and the lumen decrease was 43.7 ± 5.03 % in males and 39.12 ± 3.04 % in females, p=043. As no significant sex-related differences were observed data from both male and female were pooled together in subsequent analysis.

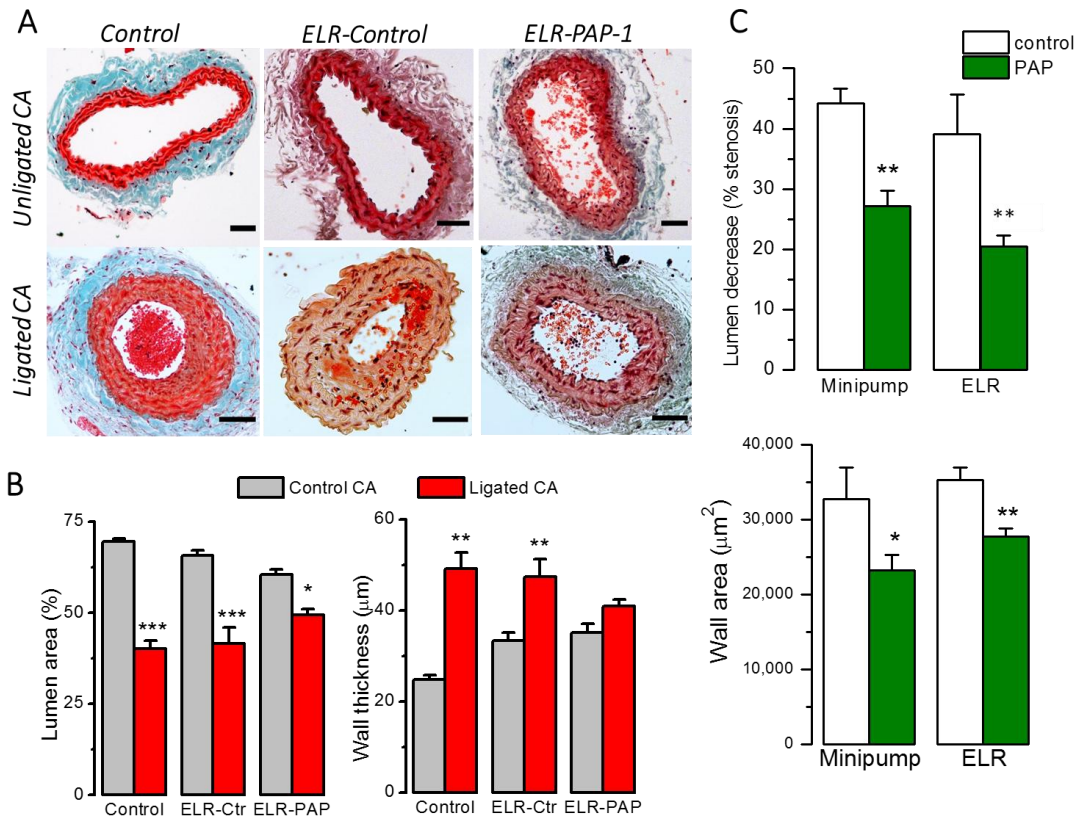

Figure 5. Effect of ELR-PAP hydrogel in an in vivo model of vascular injury. A. Representative

microphotographs of carotid arteries stained with Masson´s trichrome. Paired arteries of the same animal, left unligated carotid arteries (CA) and right ligated CA are shown. The ligated CA was left untreated or treated with ELR or ELR-PAP hydrogel as indicated (20x objective. scale bars 50 µm). **B.** The bar graphs plot the differences in lumen area and wall thickness between control, unligated (grey bars) and ligated arteries (red bars). Mean ±SEM of 5-6 animals in each group; * p<0.05; **p<0.01; *** p<0.001 for paired data. **C.** Bar plots representing % lumen decrease (upper graph) and wall area (lower one) of ligated carotid arteries. Both values were used to compare remodeling of ligated arteries between control, untreated animals (while bars) and PAP-1 treated animals (green bars) in two independent set of experiments. In the minipump experiments, the control animals were infused with vehicle, and in the ELR experiments, control animals have perivascular application of ELR-hydrogel. Analysis was performed averaging the data from 3-6 different cross section per vessel. Mean ± SEM; n=5-7 animals per group. *p<0.05; **p<0.01 compared to their own controls.

Finally, to evaluate the effect of ELR-PAP hydrogel application in the prevention of IH after carotid ligation, we compared the effects of these hydrogels with the systemic application of PAP-1 using minipumps, to release the drug over the 4-week period (Figure 5C). We found that in both cases PAP-1 application was able to significantly reduced remodeling, by decreasing both the augmented wall area and the lumen reduction. These data indicate that also in vivo the release of PAP-1 from the ELR hydrogel provides adequate therapeutic local levels of PAP-1 at the place of lesion. In addition, no significant side effects were observed in these animals in which the hydrogel was applied (with or without PAP) pointing to a good biocompatibility of these compounds as previously suggested in in vitro experiments [16,33]. The mice recovered from surgery at the same rate than the control animals (with no ELR application), and in fact their weight gain in the 4 weeks after the surgery was not different in both groups (Figure 6A). In two additional mice, sections of the whole neck were obtained to explore ELR location and looking for signs of inflammation, necrosis or any other adverse reaction. Figure 6B illustrates the unreactive nature of these compounds, which did not show any apparent harmful effect apart from some morphological disturbance due to space-occupancy effect.

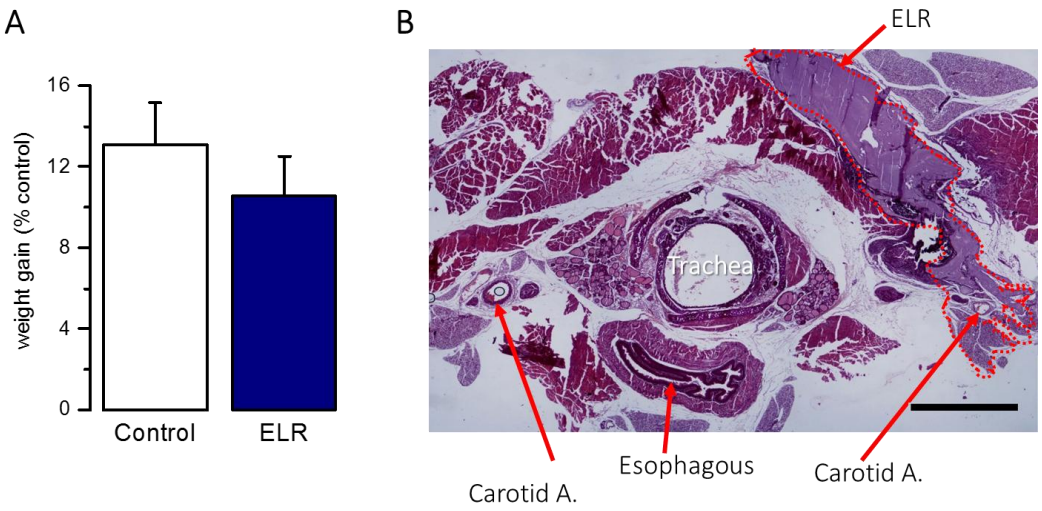

Figure 6. Absence of harmful side effects of ELR-hydrogels in vivo. A. Plot of the weight gain observed during 4 weeks (from surgery to end-point procedure) in untreated animals or animals treated with perivascular ELR hydrogels. Data are mean ± SEM of 7-10 animals per group, no significant differences were observed. **B.** Cross section of the neck of a mice obtained 4 weeks after perivascular application of ELR hydrogel around the right CA. Section was stained with Hematoxylin-eosin. The dashed line

shows the area occupied by the ELR-hydrogel. Scale bar 1 mm).

Discussion

Cardiovascular disease is the first cause of death in developed countries. However, the burden of these diseases is not confined to mortality. With statistics describing increasing levels of hospitalization and surgical intervention, their treatment may have a high economic and social cost [1]. In the case of patients with symptomatic coronary artery disease, implantation of DES releasing anti-proliferative agents had improved the outcomes of these interventions. However, DES had substantial drawbacks, including delayed healing, local hypersensitivity reactions and neoatherosclerosis, which all led to newer-generation DES with different scaffold designs, different durable and/or biodegradable polymers and new antiproliferative drug types and doses. This is a very active field of research, as >30 different DES are commercially available in Europe and USA [34]. Still, the lack of efficient anti-restenosis therapies determines the long-term failure of a substantial percentage of vascular interventions, both percutaneous and open, so that the effective restoration and maintenance of coronary vessel patency is a major problem requiring evaluation. Principle reasons for the disappointingly slow clinical implementation of these therapies are an incomplete understanding of the vascular biology of restenosis, the difficulty of translating findings in animal models into the human setting and the technical difficulties to achieve efficient drug delivery at the lesion place of the vessels.

Here we demonstrate that the combined used of a novel therapeutical target (Kv1.3 channels) and a novel scaffold as the delivery system (ELRs hydrogels) could represent a promising approach for the prevention of restenosis in human vessels. Our data provide evidence that these ELR-PAP devices, which have been tested in different formats, allowed a continuous release of PAP-1 at therapeutical levels with an appropriate time course. The small amounts of PAP-1 released make difficult to obtain a reliable determination of the free drug concentration in our experimental settings. However, our functional readout in all preparations explored indicates that both the dose and the time course of release are adequate for required tasks, which range from the inhibition of proliferation of human VSMCs in culture to the prevention of IH of human vessels in organ culture or the inhibition of remodeling in an in vivo model of vascular lesion. In this latter case, determination of free circulating PAP-1 levels along time could be pursued, but they still would not provide a better evidence than morphometric analysis, which reflect that therapeutical levels are obtained locally, at the vessel wall and in the place of injury. In fact, it has been reported that in most durable-polymer DES, the drug might continue to exist beyond the reported release profiles in levels below currently detectable limits within the polymer matrix, and these low levels of drug can have biological consequences related to vascular healing and IH inhibition [34].

The choice of these three different biological settings is not accidental but tries to uncover several relevant aspects needed to provide novel therapies capable of inhibit vessel restenosis in the clinics. 1) The *in vitro* systems demonstrates the ability of ELR hydrogels to provide therapeutical levels of PAP-1 on human VSMCs during prolonged times with no toxicity of these compounds, either as covered grids or as beads; 2) the *in vivo* model shows that PAP-1 released from the ELR hydrogels blocks IH and restenosis in the absence of toxic side effect of the ELR or the PAP-1 released; and 3) the organ culture confirms the results of the animal model in human vessels, which is not a minor point (see below).

Advantages of PAP-1 as an anti-restenosis drug.

Despite our best efforts, restenosis and in-stent stenosis are still prevalent. A large number of pharmacological agents, many of which are highly specific to their targets and have a clear anti-proliferative effect in vitro, end up failing to inhibit restenosis in the clinics. One very likely reason for this failure is that restenosis is the consequence of several overlapping biological process with different time courses and different relevance (depending on species and vascular bed). In human arteries, it is not well defined how much other processes such as inward remodeling of the vessel wall and elastic recoil, thrombus formation and reorganization and inflammatory reaction determine restenosis in addition to neointima formation [35]. Furthermore, even if neointimal formation were the major cause of restenosis, the role of cell proliferation remains controversial. Upon PM, VSMCs undergo proliferation, migration or both, followed by increased ECM synthesis resulting in the IH lesion.

According to this, an ideal anti-restenosis drug candidate should be not only an antiproliferative drug but also at least a drug that inhibits dedifferentiated VSMC, being able to block the proliferative, secretory and migratory properties of VSMCs. These functions have been confirmed for Kv1.3 channel blockers such as PAP-1 in different preparations including human vessels ([8,11], making Kv1.3 channel a good target for the prevention of IH. In addition, there is good evidence that Kv1.3 blockers can target other biological processes involved in restenosis, as they have been shown to have anti-inflammatory, anti-thrombotic and immunomodulatory effects [36–38], so that they contribute to decreased fibrosis, platelet aggregation and inflammation in the lesion. Remarkably, in comparison with the most common drugs used in DES in the clinics (namely mTOR inhibitors and paclitaxel and derivates, [35]), PAP-1 shows the additional advantage of its low systemic toxicity, which has been previously characterized [39] and extensively reported in different animal models [40–44] and also demonstrated here with the use of PAP-1 delivering minipumps.

The advantages of perivascular administration and the need for a sustained drug release

Perivascular administration combines increased efficacy with low toxicity, but no matter how restricted and controlled the drug localization is, a fraction of the drug may reach the systemic circulation by diffusion through the vessel walls. In the case of PAP-1, the absence of evident toxic side effects even when administered systemically at therapeutical doses provides an increased level of safety. Additional advantages of local (and particularly perivascular) over systemic drug release approaches are evident in the case of CABG, especially when using venous grafts [7]. Mechanical support and even constriction of the vessel to increase shear stress has been suggested as beneficial for the arterialization of the vein graft and hence to improve vessel patency [45], as external scaffolds prevented vein dilatation, decreased the development of IH and preserved the architecture of the media layer. This can be also true here, as perivascular application of ELR hydrogel significantly prevented the increased wall thickness observed upon ligation of control untreated arteries (see figures 5B and S8). The change in wall thickness between control and ligated CA was 199 ± 16 % in control mice and 148 ± 4% in ELR treated vessels ($p<0.05$). Although drug-free devices have proven their efficacy in controlling focal vascular pathologies, their efficiency is improved when active compounds are added [46–48]. In our example, wall thickness in ELR-PAP treated vessels was 116 ± 4% of control artery ($p<0.001$ compared to untreated or ELR-treated groups, Figure S8). While the choice of this compound is of utmost importance, the emphasis on delivering the compound at the right place and with the right kinetics is also critical. The drug needs to be

released with the appropriate time course, matching the development of the pathology. In the case of human saphenous veins, a sustained release over 2-4 weeks is necessary. The initial inflammatory reaction within the first 24h leads to PM of VSMCs. These cells proliferate and migrate creating an IH lesion after 2-4 weeks, which then progresses at a slower rate during the following weeks or months [6].

In this sense, drug release at the right place is feasible thanks to the hydrogel injectability at the lesion place area based in ELRs thermoresponsiveness and fast "click" interchains reaction. The click technology allows ELRs chains crosslinking at physiological conditions with no byproducts in an atom economy process. The "in situ" formation of the PAP-1 loaded hydrogel, from adequately modified ELRs and PAP-1 solutions, by a green click methodology affords biocompatible depots for perivascular administration. In this regard, the use of PAP-1 among other possible highly selective Kv1.3 blockers in the ELR hydrogel have some additional advantages, as PAP-1 is a lipophilic molecule with good tissue retention. Moreover, in vitro data show also that PAP-1 release from ELR hydrogels occurs with an adequate kinetics. The drug release profile shows an apparent delay due to the PAP-1 strong interaction with polymer chains, slowing down the diffusion process (see figure 1). Despite the low release rate, the presence of PAP-1 occurs at effective doses for more than 12 weeks (Figure 3C).

ELRs compounds releasing PAP-1 are effective in different vascular preparations

So, PAP-1 is not just another agent that inhibits VSMC proliferation *in vitro* but it is also effective inhibiting neointima formation and restenosis in the ligated carotid artery. This *in vivo* model can help to define the coordinated biological processes involved in restenosis and in the vessel response to drug therapy. Still, there are many reasons why success in animal studies may not convert to success in humans. Both the injury and the response to injury may be very different in diseased versus normal vessels and in small muscular coronary arteries versus large elastic peripheral arteries [49]. Also, while in rodent vessels there is a high contribution of VSMC proliferation and IH to restenosis, in human restenotic lesions constrictive inward remodeling is a major determinant of vessel lumen size, reflecting important qualitatively and quantitatively differences in the restenosis mechanisms [49,50]. For all these reasons, we explored the remodeling and the response to treatment of human vessels in organ culture, using saphenous vein rings donated from patients undergoing CABG. Also in this system we validate the efficiency of ELRs compounds releasing PAP-1, as the effects on remodeling did not differ from those of the free drug at submaximal concentrations [8]. Although the organ culture is not a whole vessel system in situ, thus lacking some important mechanical and chemical regulatory mechanisms, it offers the advantage to explore IH development and its response to treatment in the same vessels of the same patients undergoing vascular surgery for coronary artery disease. As ELRs have been already proposed as well-suited scaffolds for coating stents, altogether, our results indicate that their use in combination with PAP-1 as the active released anti-restenotic agent offers important advantages for the treatment of unwanted remodeling after vascular interventions.

Acknowledgements

We want to thank Esperanza Alonso for excellent technical assistance. We are in debt with Drs A. San Román, Mirella Fernandez, and all the personnel of the Cardiac Surgery Unit of the Hospital Clínico Universitario de Valladolid for their wiliness to provide all the vessel samples for this study. We are also grateful to COLMAH (COLección de Muestras Arteriales Humanas)

collection for the use of human primary VSMC cultures and to all the members of the laboratory for their helpful discussions.

The authors are grateful for financial support from the European Social Fund (ESF) and the European Regional Development Fund (ERDF), as well as grants from the EU H2020-NMP-2014-646075), the Spanish Ministerio de Economia y Competitividad MINECO (grants BFU2016-75360-R, DTS19/00162, MAT2016-79435-R, MAT2016-78903-R and RTI2018-096320-B-C22), the Junta de Castilla y León (grantst VA114P17 and VA317P18), the CIBER-BBN, the JCyL and the Instituto de Salud Carlos III under the "Network Center of Regenerative Medicine and Cellular Therapy of Castilla and Leon". S. Moreno-Estar and S. Serrano are predoctoral fellows of the Junta de Castilla y León and M. Arévalo-Martínez is predoctoral fellow of UVa-Santander

AUTHOR CONTRIBUTIONS (CRedIT roles)

Conceptualization, MS, JRLL, MTPG and FJA; Methodology: PC, MTPG and FJA, Formal Analysis: SME, SS, PC, MS and MTPG; Investigation: SME, SS, MAM, PC, JRLL. MS, MTPG and FJA; Writing – Review & Editing: SME, SS, JRLL, MS, MTPG and FJA; Visualization: SME, SS, MS, MTPG; Supervision: PC, JRLL, MS, MTPG and FJA; Funding Acquisition: JRLL, MTPG and FJA

References

[1] N. M, T. N, S. P, R. M, Cardiovascular disease in Europe: epidemiological update, Eur Hear. J. 34 (n.d.) 3028–3034.

[2] M.R. Alexander, G.K. Owens, Epigenetic Control of Smooth Muscle Cell Differentiation and Phenotypic Switching in Vascular Development and Disease, Annu. Rev. Physiol. 74 (2012) 13–40. https://doi.org/10.1146/annurev-physiol-012110-142315.

[3] R.A. Byrne, M. Joner, A. Kastrati, Stent thrombosis and restenosis: What have we learned and where are we going? the Andreas Grüntzig Lecture ESC 2014, Eur. Heart J. 36 (2015) 3320–3331. https://doi.org/10.1093/eurheartj/ehv511.

[4] K.A. Eagle, R.A. Guyton, R. Davidoff, F.H. Edwards, G.A. Ewy, T.J. Gardner, J.C. Hart, H.C. Herrmann, L.D. Hillis, A.M. Hutter, B.W. Lytle, R.A. Marlow, W.C. Nugent, T.A. Orszulak, E.M. Antman, S.C. Smith, J.S. Alpert, J.L. Anderson, D.P. Faxon, V. Fuster, R.J. Gibbons, G. Gregoratos, J.L. Halperin, L.F. Hiratzka, S.A. Hunt, A.K. Jacobs, J.P. Ornato, American College of Cardiology/American Heart Association Task Force on Practice Guidelines Committee to Update the 1999 Guidelines for Coronary Artery Bypass Graft Surgery, American Society for Thoracic Surgery, Society of Thoracic Surgeons, ACC/AHA 2004 guideline update for coronary artery bypass graft surgery: summary article. A report of the American College of Cardiology/American Heart Association Task Force on Practice Guidelines (Committee to Update the 1999 Guidelines for Coronary Artery Bypass Graft Surgery)., J. Am. Coll. Cardiol. 44 (2004) e213-310. https://doi.org/10.1016/j.jacc.2004.07.021.

[5] K. Wadey, J. Lopes, M. Bendeck, S. George, Role of smooth muscle cells in coronary artery bypass grafting failure, Cardiovasc. Res. 114 (2018) 601–610. https://doi.org/10.1093/cvr/cvy021.

[6] C.D. Owens, W.J. Gasper, A.S. Rahman, M.S. Conte, Vein graft failure, J. Vasc. Surg. 61 (2015) 203–216. https://doi.org/10.1016/j.jvs.2013.08.019.

[7] I. Mylonaki, É. Allémann, F. Saucy, J.A. Haefliger, F. Delie, O. Jordan, Perivascular medical devices and drug delivery systems: Making the right choices, Biomaterials. 128 (2017) 56–68. https://doi.org/10.1016/j.biomaterials.2017.02.028.

[8] P. Cidad, A. Moreno-Domínguez, L. Novensá, M. Roqué, L. Barquín, M. Heras, M.T.T. Pérez-García, J.R.J.R. López-López, Characterization of ion channels involved in the proliferative response of femoral artery smooth muscle cells, Arterioscler. Thromb. Vasc. Biol. 30 (2010) 1203–11. https://doi.org/10.1161/ATVBAHA.110.205187.

[9] A. Cheong, J. Li, P. Sukumar, B. Kumar, F. Zeng, K. Riches, C. Munsch, I.C. Wood, K.E. Porter, D.J. Beech, Potent suppression of vascular smooth muscle cell migration and human neointimal hyperplasia by KV1.3 channel blockers, Cardiovasc. Res. 89 (2011) 282–289. https://doi.org/10.1093/cvr/cvq305.

[10] P. Cidad, E. Miguel-Velado, C. Ruiz-McDavitt, E. Alonso, L. Jiménez-Pérez, A. Asuaje, Y. Carmona, D. García-Arribas, J. López, Y. Marroquín, M. Fernández, M. Roqué, M.T. Pérez-García, J.R. López-López, Kv1.3 channels modulate human vascular smooth muscle cells proliferation independently of mTOR signaling pathway, Pflügers Arch. - Eur. J. Physiol. 467 (2015) 1711–1722. https://doi.org/10.1007/s00424-014-1607-y.

[11] M. Arévalo-Martínez, P. Cidad, N. García-Mateo, S. Moreno-Estar, J. Serna, M.

Fernández, K. Swärd, M. Simarro, M.A. De La Fuente, J.R. López-López, M.T. Pérez-García, Myocardin-Dependent Kv1.5 Channel Expression Prevents Phenotypic Modulation of Human Vessels in Organ Culture, Arterioscler. Thromb. Vasc. Biol. 39 (2019) E273–E286. https://doi.org/10.1161/ATVBAHA.119.313492.

[12] A. Schmitz, A. Sankaranarayanan, P. Azam, K. Schmidt-Lassen, D. Homerick, W. Hansel, H. Wulff, Design of PAP-1, a selective small molecule Kv1.3 blocker, for the suppression of effector memory T cells in autoimmune diseases., Mol. Pharmacol. 68 (2005) 1254–1270. https://doi.org/10.1124/mol.105.015669.nally.

[13] J. Gonzalez-Valdivieso, B. Borrego, A. Girotti, S. Moreno, A. Brun, J.F. Bermejo-Martin, F.J. Arias, A DNA Vaccine Delivery Platform Based on Elastin-Like Recombinamer Nanosystems for Rift Valley Fever Virus, Mol. Pharm. (2020). https://doi.org/10.1021/acs.molpharmaceut.0c00054.

[14] A. Girotti, D. Orbanic, A. Ibáñez-Fonseca, C. Gonzalez-Obeso, J.C. Rodríguez-Cabello, Recombinant Technology in the Development of Materials and Systems for Soft-Tissue Repair, Adv. Healthc. Mater. 4 (2015) 2423–2455. https://doi.org/10.1002/adhm.201500152.

[15] F.J. Arias, M. Santos, A. Ibanez-Fonseca, M.J. Pina, S. Serrano, Elastin-Like Recombinamers As Smart Drug Delivery Systems, Curr. Drug Targets. 19 (2016) 360–379. https://doi.org/10.2174/1389450117666160201114617.

[16] I. González De Torre, M. Santos, L. Quintanilla, A. Testera, M. Alonso, J.C. Rodríguez Cabello, Elastin-like recombinamer catalyst-free click gels: Characterization of poroelastic and intrinsic viscoelastic properties, Acta Biomater. 10 (2014) 2495–2505. https://doi.org/10.1016/j.actbio.2014.02.006.

[17] I.G. De Torre, F. Wolf, M. Santos, L. Rongen, M. Alonso, S. Jockenhoevel, J. C.Rodríguez-Cabello, P. Mela, Elastin-like recombinamer-covered stents: Towards a fully biocompatible and non-thrombogenic device for cardiovascular diseases, Acta Biomater. 12 (2015) 146–155. https://doi.org/10.1016/j.actbio.2014.10.029.

[18] A. Fernández-Colino, F. Wolf, R. Moreira, S. Rütten, T. Schmitz-Rode, J.C. Rodríguez-Cabello, S. Jockenhoevel, P. Mela, Layer-by-layer biofabrication of coronary covered stents with clickable elastin-like recombinamers, Eur. Polym. J. 121 (2019) 109334. https://doi.org/10.1016/j.eurpolymj.2019.109334.

[19] W.E. Hennink, C.F. Van Nostrum, Novel crosslinking methods to design hydrogels, Adv. Drug Deliv. Rev. 54 (2002) 13–36. https://doi.org/10.1016/S0169-409X(01)00240-X.

[20] J.L. Schaal, X. Li, E. Mastria, J. Bhattacharyya, M.R. Zalutsky, A. Chilkoti, W. Liu, Injectable polypeptide micelles that form radiation crosslinked hydrogels in situ for intratumoral radiotherapy, J. Control. Release. 228 (2016) 58–66. https://doi.org/10.1016/j.jconrel.2016.02.040.

[21] B.C. Dash, D. Thomas, M. Monaghan, O. Carroll, X. Chen, K. Woodhouse, T. O'Brien, A. Pandit, An injectable elastin-based gene delivery platform for dose-dependent modulation of angiogenesis and inflammation for critical limb ischemia, Biomaterials. 65 (2015) 126–139. https://doi.org/10.1016/j.biomaterials.2015.06.037.

[22] T. Flora, I.G. de Torre, M. Alonso, J.C. Rodríguez-Cabello, Tethering QK peptide to enhance angiogenesis in elastin-like recombinamer (ELR) hydrogels, J. Mater. Sci. Mater. Med. 30 (2019) 1–12. https://doi.org/10.1007/s10856-019-6232-z.

[23] N.A. Peppas, Analysis of Fickian and non-Fickian drug release from polymers., Pharm. Acta Helv. 60 (1985) 110–111.

[24] E. Miguel-Velado, A. Moreno-Domínguez, O. Colinas, P. Cidad, M. Heras, M.T.T. Pérez-García, J.R.J.R. López-López, Contribution of Kv channels to phenotypic remodeling of human uterine artery smooth muscle cells, Circ. Res. 97 (2005) 1280–1287. https://doi.org/10.1161/01.RES.0000194322.91255.13.

[25] M. Roque, J.T. Fallon, J.J. Badimon, W.X. Zhang, M.B. Taubman, E.D. Reis, Mouse model of femoral artery denudation injury associated with the rapid accumulation of adhesion molecules on the luminal surface and recruitment of neutrophils., Arterioscler. Thromb. Vasc. Biol. 20 (2000) 335–342. https://doi.org/10.1161/01.ATV.20.2.335.

[26] F. Cipriani, B. Ariño Palao, I. Gonzalez de Torre, A. Vega Castrillo, H.J. Aguado Hernández, M. Alonso Rodrigo, A.J. Àlvarez Barcia, A. Sanchez, V. García Diaz, M. Lopez Peña, J.C. Rodriguez-Cabello, An elastin-like recombinamer-based bioactive hydrogel embedded with mesenchymal stromal cells as an injectable scaffold for osteochondral repair, Regen. Biomater. 6 (2019) 335–347. https://doi.org/10.1093/rb/rbz023.

[27] T.K.L. Meyvis, B.G. Stubbe, M.J. Van Steenbergen, W.E. Hennink, S.C. De Smedt, J. Demeester, A comparison between the use of dynamic mechanical analysis and oscillatory shear rheometry for the characterisation of hydrogels, Int. J. Pharm. 244 (2002) 163–168. https://doi.org/10.1016/S0378-5173(02)00328-9.

[28] G.M. Ravanagh, S.B. Ross-Murphy, RHEOLOGICAL CHARACTERISATION OF POLYMER GELS, 1998.

[29] N.W. Tschoegl, The phenomenological theory of linear viscoelastic behavior: an introduction, Springer, 1989. http://scholar.google.com/scholar?hl=en&btnG=Search&q=intitle:the+phenomenological+theory+of+linear+viscoelastic+behavior+an+introduction#0 (accessed May 3, 2020).

[30] L. Zhang, H. Cheng, C. Zheng, F. Dong, S. Man, Y. Dai, P. Yu, Structural and release properties of amylose inclusion complexes with ibuprofen, J. Drug Deliv. Sci. Technol. 31 (2016) 101–107. https://doi.org/10.1016/j.jddst.2015.12.006.

[31] M. V. Natu, M.H. Gil, H.C. de Sousa, Supercritical solvent impregnation of poly(ε-caprolactone)/poly(oxyethylene-b-oxypropylene-b-oxyethylene) and poly(ε-caprolactone)/poly(ethylene-vinyl acetate) blends for controlled release applications, J. Supercrit. Fluids. 47 (2008) 93–102. https://doi.org/10.1016/j.supflu.2008.05.006.

[32] A. Kumar, V. Lindner, Remodeling With Neointima Formation in the Mouse Carotid Artery After Cessation of Blood Flow, Arterioscler. Thromb. Vasc. Biol. 17 (1997) 2238–2244. https://doi.org/10.1161/01.ATV.17.10.2238.

[33] I.G. De Torre, F. Wolf, M. Santos, L. Rongen, M. Alonso, S. Jockenhoevel, J. C.Rodríguez-Cabello, P. Mela, Elastin-like recombinamer-covered stents: Towards a fully biocompatible and non-thrombogenic device for cardiovascular diseases, Acta Biomater. (2015). https://doi.org/10.1016/j.actbio.2014.10.029.

[34] S. Torii, H. Jinnouchi, A. Sakamoto, M. Kutyna, A. Cornelissen, S. Kuntz, L. Guo, H. Mori, E. Harari, K.H. Paek, R. Fernandez, D. Chahal, M.E. Romero, F.D. Kolodgie, A. Gupta, R. Virmani, A. V. Finn, Drug-eluting coronary stents: insights from preclinical and pathology studies, Nat. Rev. Cardiol. 17 (2020) 37–51. https://doi.org/10.1038/s41569-019-0234-x.

[35] M.R. Bennett, In-stent stenosis: Pathology and implications for the development of drug eluting stents, Heart. 89 (2003) 218–224. https://doi.org/10.1136/heart.89.2.218.

[36] S. Feske, H. Wulff, E.Y. Skolnik, Ion channels in innate and adaptive immunity., Annu. Rev. Immunol. 33 (2015) 291–353. https://doi.org/10.1146/annurev-immunol-032414-112212.

[37] C. McCloskey, S. Jones, S. Amisten, R.T. Snowden, L.K. Kaczmarek, D. Erlinge, A.H. Goodall, I.D. Forsythe, M.P. Mahaut-Smith, Kv1.3 is the exclusive voltage-gated K+ channel of platelets and megakaryocytes: roles in membrane potential, Ca2+ signalling and platelet count., J. Physiol. 588 (2010) 1399–406. https://doi.org/10.1113/jphysiol.2010.188136.

[38] R. Vicente, A. Escalada, M. Coma, G. Fuster, E. Sánchez-Tilló, C. López-Iglesias, C. Soler, C. Solsona, A. Celada, A. Felipe, Differential voltage-dependent K+ channel responses during proliferation and activation in macrophages., J. Biol. Chem. 278 (2003) 46307–20. https://doi.org/10.1074/jbc.M304388200.

[39] B. Hao, Z.W. Chen, X.J. Zhou, P.I. Zimin, G.P. Miljanich, H. Wulff, Y.X. Wang, Identification of phase-I metabolites and chronic toxicity study of the Kv1.3 blocker PAP-1 (5-(4-phenoxybutoxy)psoralen) in the rat, Xenobiotica. 41 (2011) 198–211. https://doi.org/10.3109/00498254.2010.532886.

[40] L.E. Pereira, F. Villinger, H. Wulff, A. Sankaranarayanan, G. Raman, A.A. Ansari, Pharmacokinetics, toxicity, and functional studies of the selective Kv1.3 channel blocker 5-(4-phenoxybutoxy)psoralen in rhesus macaques., Exp. Biol. Med. (Maywood). 232 (2007) 1338–54. https://doi.org/10.3181/0705-RM-148.

[41] J. Di Lucente, H.M. Nguyen, H. Wulff, L.-W. Jin, I. Maezawa, The voltage-gated potassium channel Kv1.3 is required for microglial pro-inflammatory activation *in vivo*, Glia. 66 (2018) 1881–1895. https://doi.org/10.1002/glia.23457.

[42] X. Wu, R. Xu, M. Cao, L. Ruan, X. Wang, C. Zhang, Effect of the Kv1.3 voltage-gated potassium channel blocker PAP-1 on the initiation and progress of atherosclerosis in a rat model, Heart Vessels. 30 (2015) 108–114. https://doi.org/10.1007/s00380-013-0462-7.

[43] Y. Mei, C. Fang, S. Ding, X. Liu, J. Hu, J. Xu, Q. Mei, PAP-1 ameliorates DSS-induced colitis with involvement of NLRP3 inflammasome pathway, Int. Immunopharmacol. 75 (2019) 105776. https://doi.org/10.1016/j.intimp.2019.105776.

[44] S. Kundu-Raychaudhuri, Y.J. Chen, H. Wulff, S.P. Raychaudhuri, Kv1.3 in psoriatic disease: PAP-1, a small molecule inhibitor of Kv1.3 is effective in the SCID mouse psoriasis - Xenograft model, J. Autoimmun. 55 (2015) 63–72. https://doi.org/10.1016/j.jaut.2014.07.003.

[45] A. Longchamp, F. Alonso, C. Dubuis, F. Allagnat, X. Berard, P. Meda, F. Saucy, J.M. Corpataux, Sébastien Déglise, J.A. Haefliger, The use of external mesh reinforcement to reduce intimal hyperplasia and preserve the structure of human saphenous veins, Biomaterials. 35 (2014) 2588–2599. https://doi.org/10.1016/j.biomaterials.2013.12.041.

[46] I. Skalský, O. Szárszoi, E. Filová, M. Pařízek, A. Lytvynets, J. Malušková, A. Lodererová, E. Brynda, V. Lisá, Z. Burdíková, M. Čapek, J. Pirk, L. Bačáková, A perivascular system releasing sirolimus prevented intimal hyperplasia in a rabbit model in a medium-term study, Int. J. Pharm. 427 (2012) 311–319.

https://doi.org/10.1016/j.ijpharm.2012.02.023.

[47] I. Mylonaki, O. Trosi, E. Allémann, M. Durand, O. Jordan, F. Delie, Design and characterization of a perivascular PLGA coated PET mesh sustaining the release of atorvastatin for the prevention of intimal hyperplasia, Int. J. Pharm. 537 (2018) 40–47. https://doi.org/10.1016/j.ijpharm.2017.12.026.

[48] D. Wiedemann, A. Kocher, N. Bonaros, S. Semsroth, G. Laufer, M. Grimm, T. Schachner, Perivascular administration of drugs and genes as a means of reducing vein graft failure, Curr. Opin. Pharmacol. 12 (2012) 203–216. https://doi.org/10.1016/j.coph.2012.02.012.

[49] M.R. Bennett, M.O. Sullivan, Mechanisms of angioplasty and stent restenosis : implications for design of rational therapy, 91 (2001) 149–166.

[50] S.A. Goel, L.-W. Guo, B. Liu, K.C. Kent, Mechanisms of post-intervention arterial remodelling, (n.d.). https://doi.org/10.1093/cvr/cvs276.

Figures1-6

Click here to download Figure: Moreno-Estar et al. All figures.pdf

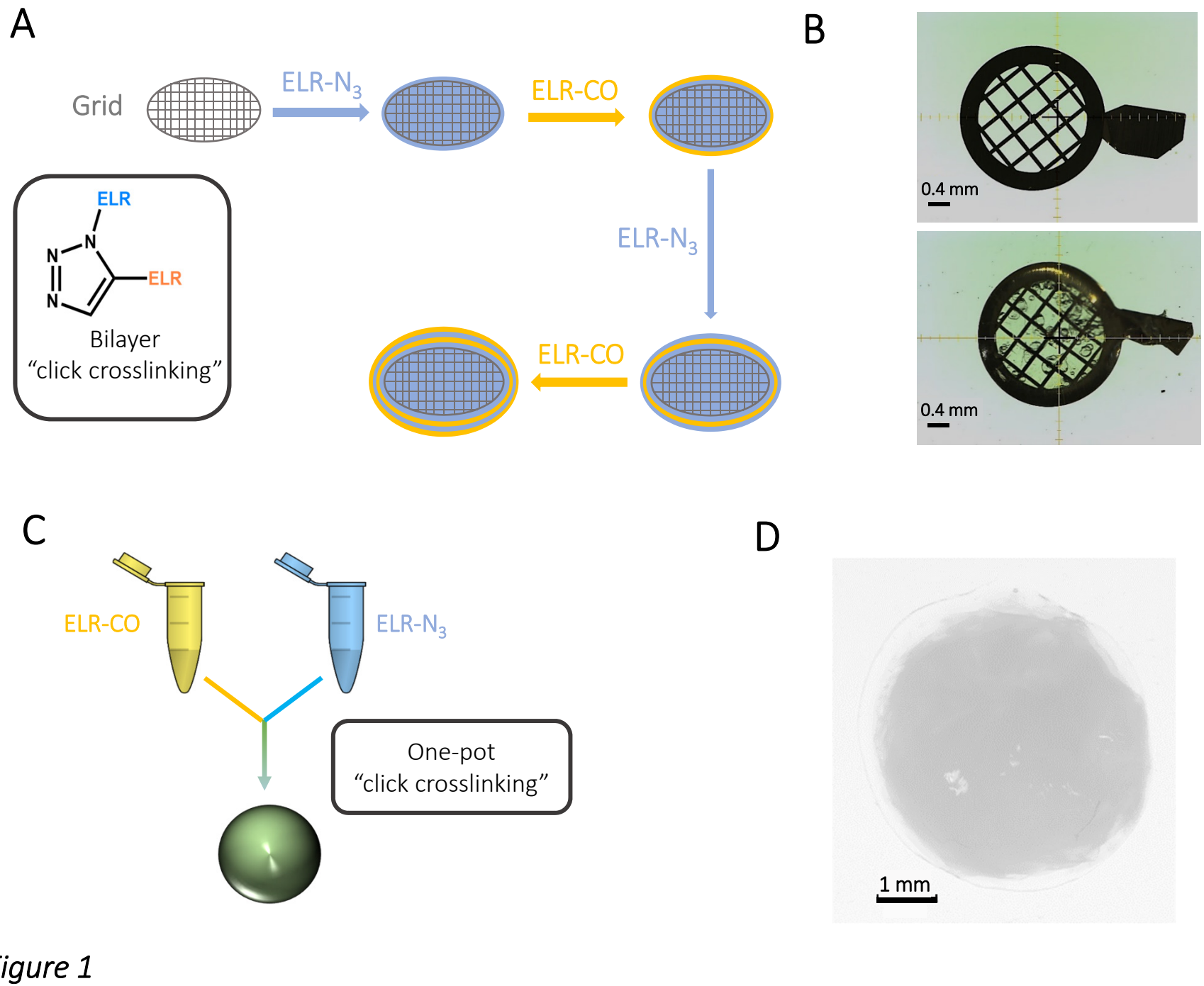

Figure 1

A

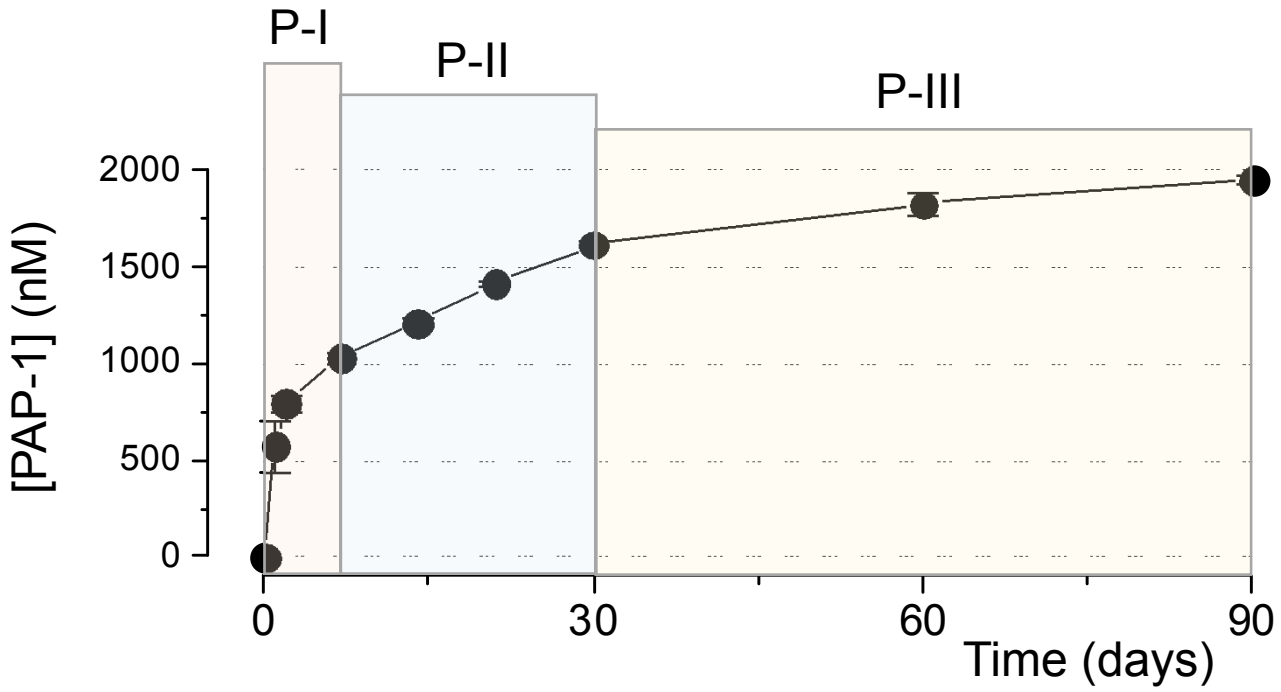

B

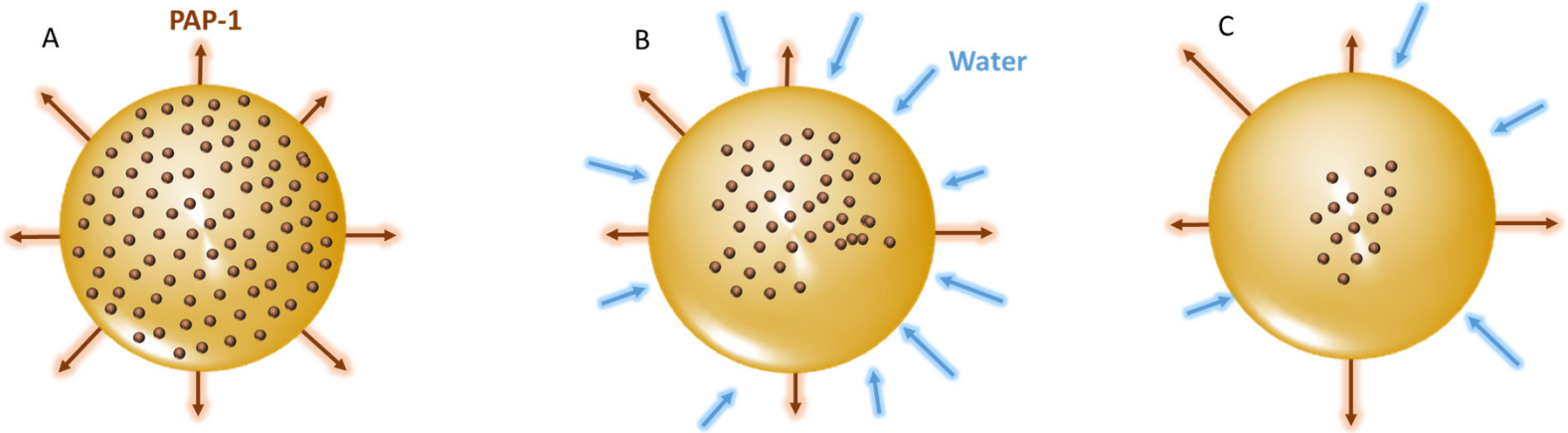

First period (0-7 day).
Anomalous transport

Second period (7-30 days).
Pseudo-Fickian diffusion

Third period (30-90 days).
Pseudo-Fickian diffusion.

Figure 2

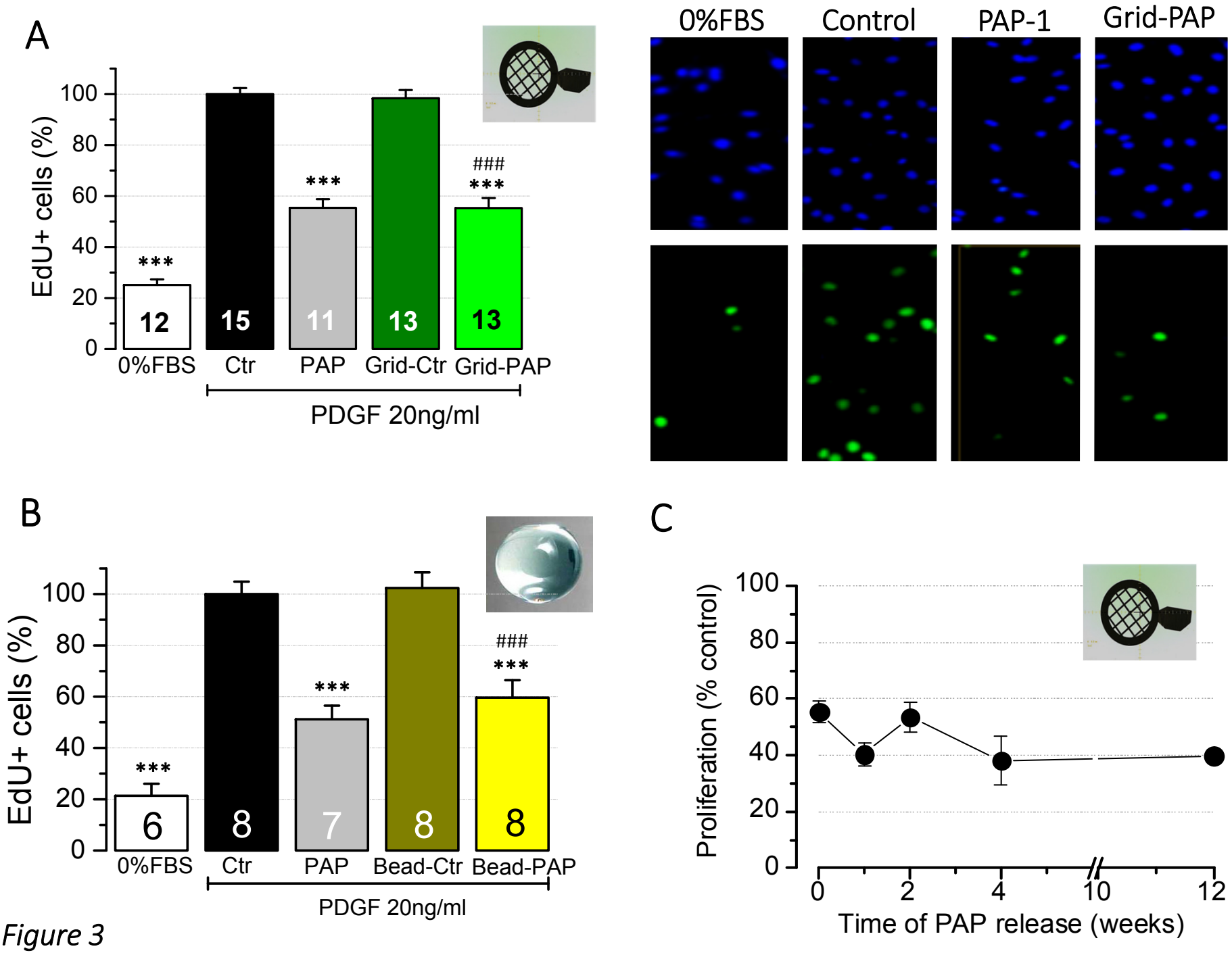
A
EdU+ cells (%)
100
80
60
40
20
0
***
12
15
11
13
13
***
###
***
0%FBS
Ctr
PAP
Grid-Ctr
Grid-PAP
PDGF 20ng/ml
0%FBS
Control
PAP-1
Grid-PAP
B
EdU+ cells (%)
100
80
60
40
20
0
***
6
8
7
8
8
***
###
***
0%FBS
Ctr
PAP
Bead-Ctr
Bead-PAP
PDGF 20ng/ml
C
Proliferation (% control)
100
80
60
40
20
0
0
2
4
10
12
Time of PAP release (weeks)

Figure 3

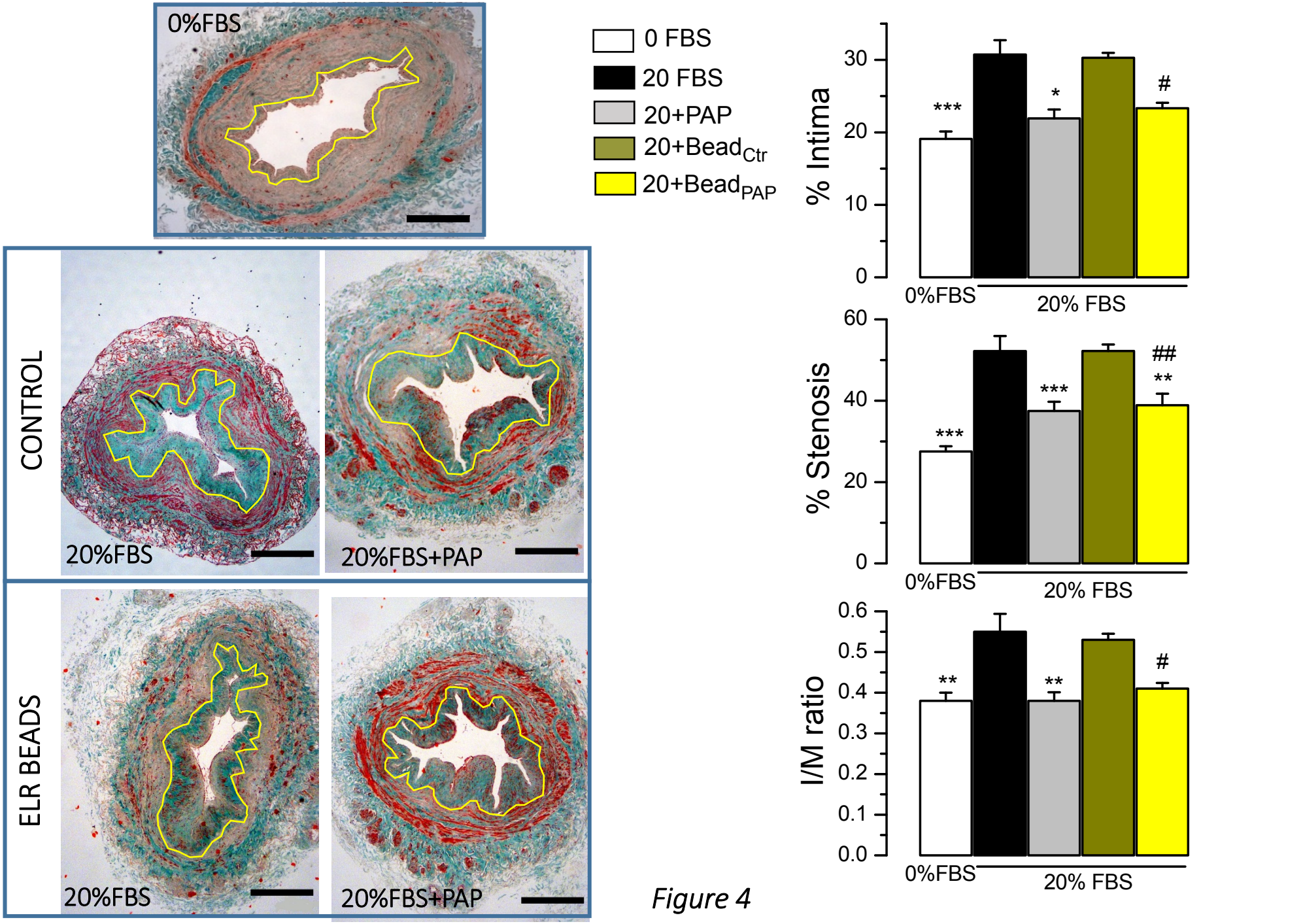
0%FBS
CONTROL
20%FBS
20%FBS+PAP
ELR BEADS
20%FBS
20%FBS+PAP
0 FBS
20 FBS
20+PAP
20+Bead$_{Ctr}$
20+Bead$_{PAP}$
% Intima
% Stenosis
I/M ratio
0%FBS
20% FBS
***
*
#
***
***
##
**
**
**
#

Figure 4

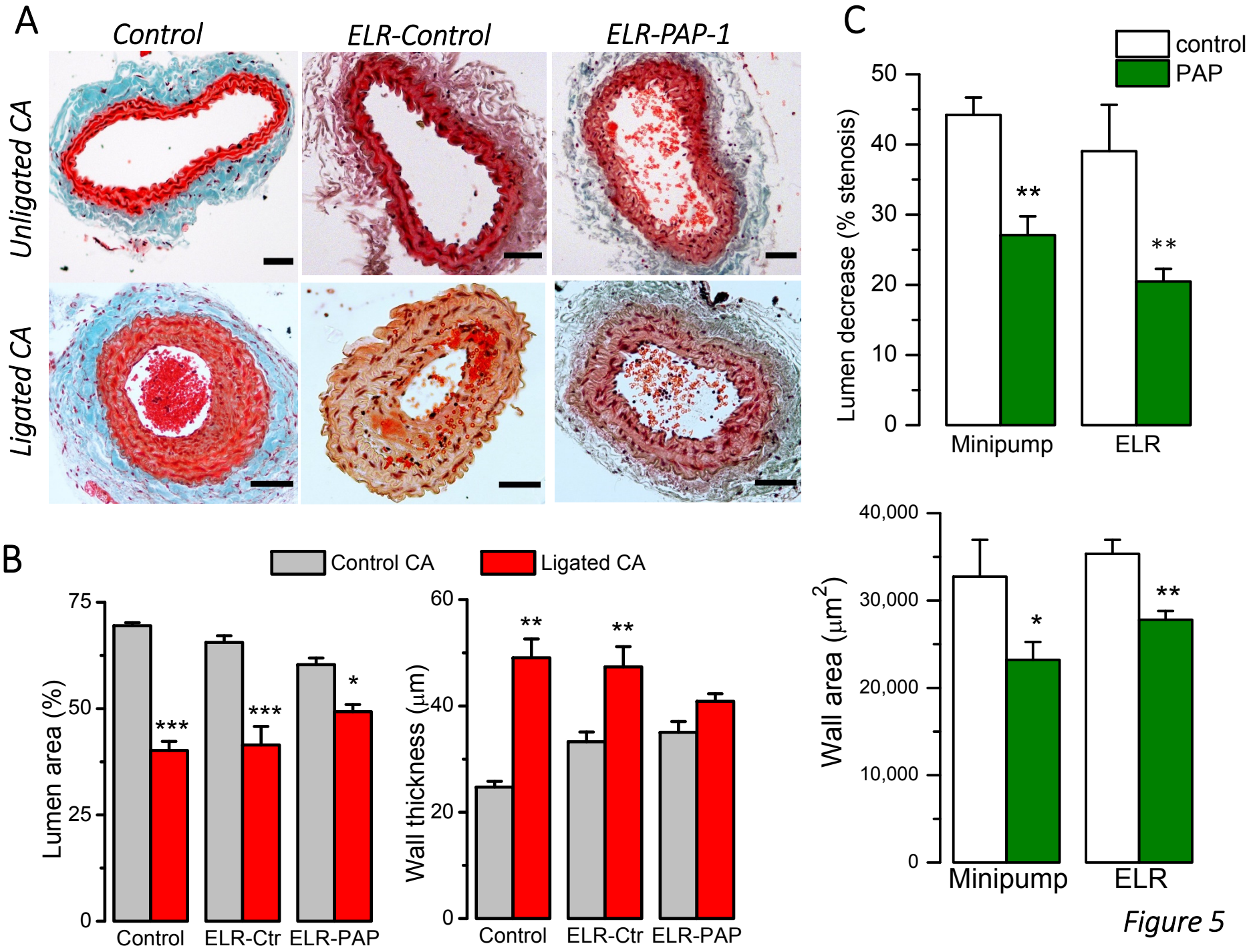
A
Control
ELR-Control
ELR-PAP-1
Unligated CA
Ligated CA
B
Control CA
Ligated CA
Lumen area (%)
75
50
25
0
***
***
*
Control
ELR-Ctr
ELR-PAP
Wall thickness (μm)
60
40
20
0
**
**
Control
ELR-Ctr
ELR-PAP
C
control
PAP
Lumen decrease (% stenosis)
50
40
30
20
10
0
**
**
Minipump
ELR
Wall area (μm2)
40,000
30,000
20,000
10,000
0
*
**
Minipump
ELR

Figure 5

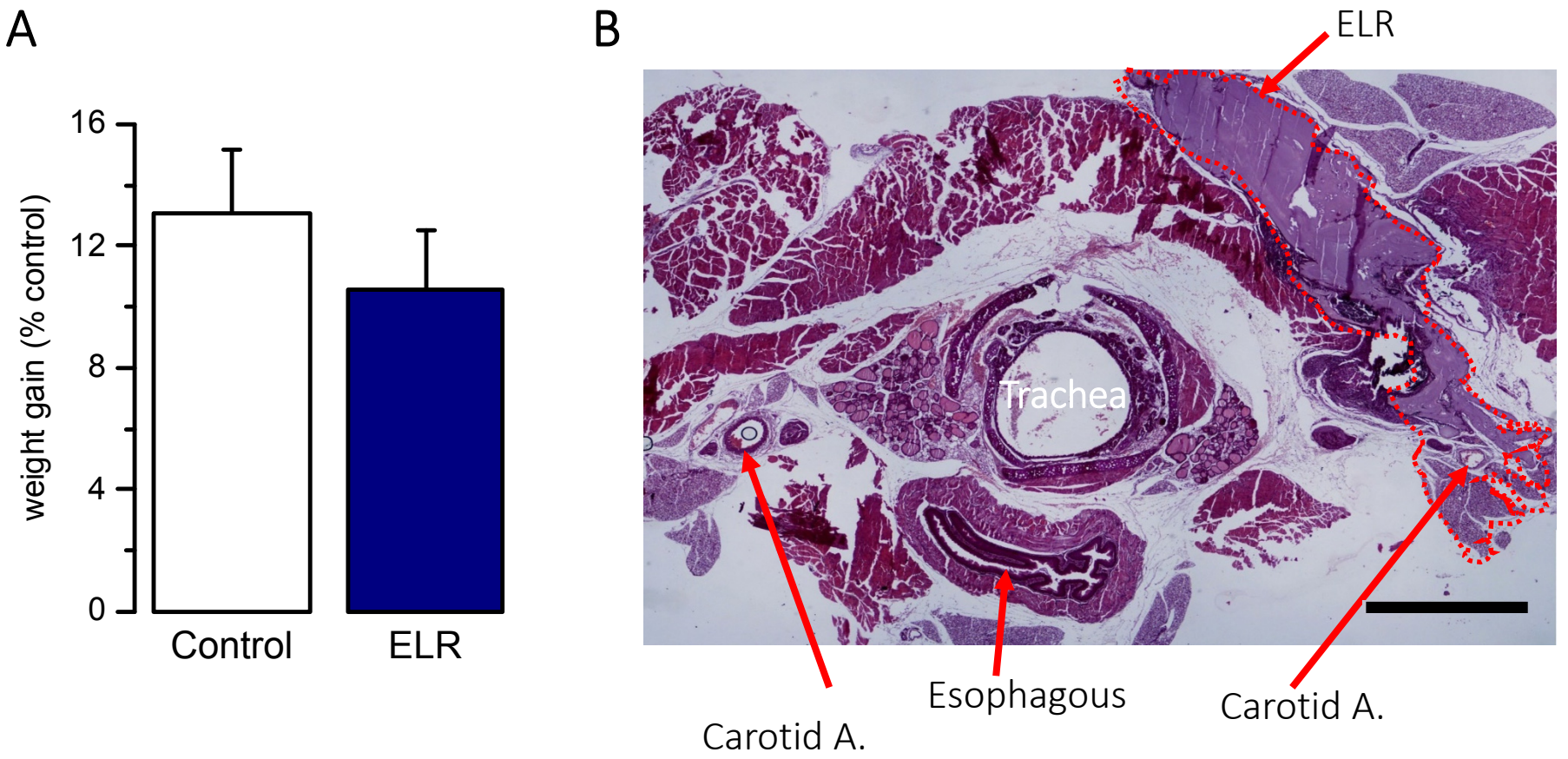
A
16
12
8
4
0
weight gain (% control)
Control
ELR
B
ELR
Trachea
Carotid A.
Esophagous
Carotid A.

Figure 6